Available on CMS information server

CMS NOTE 2003/020

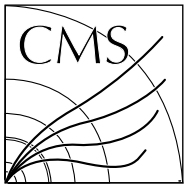

The Compact Muon Solenoid Experiment

CMS Note

Mailing address: CMS CERN, CH-1211 GENEVA 23, Switzerland

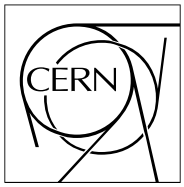

Sensor design for the CMS Silicon Strip Tracker

L. Borrello, A. Messineo

Università degli Studi di Pisa and INFN Pisa

E. Focardi, A. Macchiolo

Università degli Studi di Firenze and INFN Firenze

Abstract

The Silicon Strip Tracker (SST) constitutes, in conjunction with the Pixel Detector, the inner tracking system of the Compact Muon Solenoid (CMS) experiment. The SST consists of about 24000 rectangular and wedge-shaped silicon sensors, designed in 15 different geometries. The active area instrumented with silicon sensors is of 198 m^2 and the total number of read-out channels is 9.6 Million. This note is aimed to describe the design of the silicon sensors, for the different detector topologies foreseen by the SST.

1 General design features

The CMS tracking system is fully based on silicon detector technology [1] [2]. The Silicon Strip Tracker (SST) is equipped with 24244 single-sided micro-strip sensors covering an active area of 198 m^2.
The sensors are manufactured using 6" technology, with the standard planar process usually employed in the Integrated Circuit (IC) industry. One single detector is produced from each wafer and it is requested to lie inside a fiducial circle of about 13.9 cm diameter. The crystal lattice orientation is of <100> type [3].
The wafer thickness is required to be 320 μm for "thin" sensors, with a substrate resistivity in the range 1.5÷ 3.25 KΩcm, and 500 μm for "thick" sensors, with a requested resistivity of 4÷ 8 KΩcm [2]. Thick sensors will be supplied to the Tracker Collaboration by ST Microelectronics (STM) and thin sensors by Hamamatsu Photonics (HPK).
The thickness must be within 20 μm of the specification and the flatness such that the sensor warp over its total lenght is less than 100 μm. The requested dicing accuracy for the main sensor is at the level of 20 μm. The mask alignment tolerance and the requested precision of the implant dimensions are one μm.

A schematic cross-section of the detector active region is shown in Fig.1.

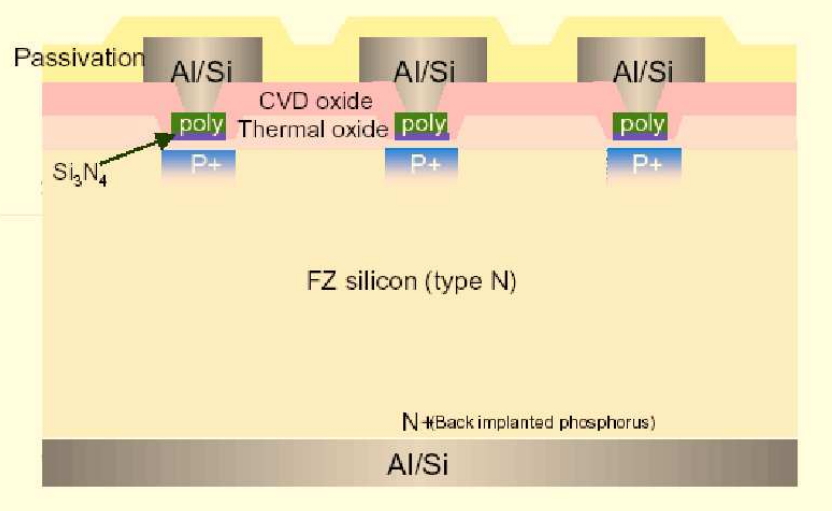

Figure 1: Schematics of a section of an STM detector (junction side on the top of the figure, ohmic side on the bottom).

A uniformly metallized n^+ layer is implanted on the sensor back-side providing an ohmic contact between the bulk and the metal layer. Moreover, the presence of this highly doped n^+ layer acts as a barrier for minority carriers coming from the depleted bulk and for majority carriers injected from the metal contacts, keeping the overall leakage current very low. In addition, on the junction side, an n^+ implantation is required along the edges of the device, in order to prevent the space charge region from reaching the cutting edge. This implantation, covered by an aluminum layer, helps to protect the active area from the injection of charges originating in this heavily damaged region.
The passivation of the front side improves the detector stability and reduces the handling fragility. The producers are requested to supply sensors polished in the front and acid etched in the back-side.
The active region is surrounded by two p^+ implanted rings covered by an aluminum layer. The external one (guard ring), left floating, helps to gradually degrade the field between the n^+ implantation at the sensor edges, and the internal p^+ ring (bias ring), which is connected to ground and is used to bias the strips. The metal field plates extend beyond the implantation, to avoid high fields at its edge. The ring geometry and the large metal over-hang on the external side of the guard ring help to avoid critical electric field configuration while operating the device at high voltage [3] [4].
The bias and guard rings are wider in the direction perpendicular to the strips to simplify testing and biasing procedures.
In order to minimize the occurrence of breakdown phenomena the distance between the active area and the cutting edge has been chosen equal to twice the thickness plus 110 μm.
In the active region a p^+ implantation is used on the front side to define the strip-shaped diode. On top of each strip an integrated capacitor is built for signal read-out. The capacitor consists of a multiple layer of dielectrics

covered by a metal layer.
The width of the implanted strips depends on the strip pitch: a constant width/pitch of 0.25 is used for all the sensor geometries [3]. This value is a compromise between a high width/pitch ratio that reduces the field peak located at the p^+ edge and a low value of the ratio that keeps the total strip capacitance low.
The two producers are left free to choose the appropriate technology for the integrated coupling capacitors provided that they are able to satisfy the requirements on the number of defective strips (at the percent level). Both manufacturers have implemented multiple thin layers of SiO_2 and Si_3N_4. A thicker oxide fills the inter-strip gap.
The aluminum read-out strips, capacitively coupled over the p^+-implants, will be on both sides 15 % wider than the width of the implantation underneath. The overhang ranges from a minimum of 4 μm to a maximum of 8 μm, depending on the strip pitch. As in the case of the bias and guard rings, this design choice will move the high electric field region from the silicon into the oxide layer, reducing the risk of electrical breakdown [3] [4]. The thickness of the metal layer is required to be greater than 1.2 μm to limit the noise contribution due to the resistance of the electrode.
An array of poly-silicon resistors, with a resistance value requested to be 1.5 $\pm$ 0.5 MΩ, is used to bias the implanted strips. The design foresees a wiggled shape to provide the required resistance values in a compact format. The resistors are aligned on the same side of the sensor and they connect the bias ring to the corresponding p^+-implant of the strip through a metallized probe pad (DC pad). The choice of poly-silicon as biasing technique is mainly due to its established radiation resistance, and it relies on the capability of producers in defining the resistance value by means of controlled doping by implantation or diffusion.
Two rows of AC pads are used at the ends of the strips on each side of the detector to allow for bonding and testing. In the rectangular sensors and in most of the wedge-shaped ones, the pad pitch has been kept constant. An example of how the different structures are arranged in the active region is shown in Fig. 2. A series of L-shaped reference

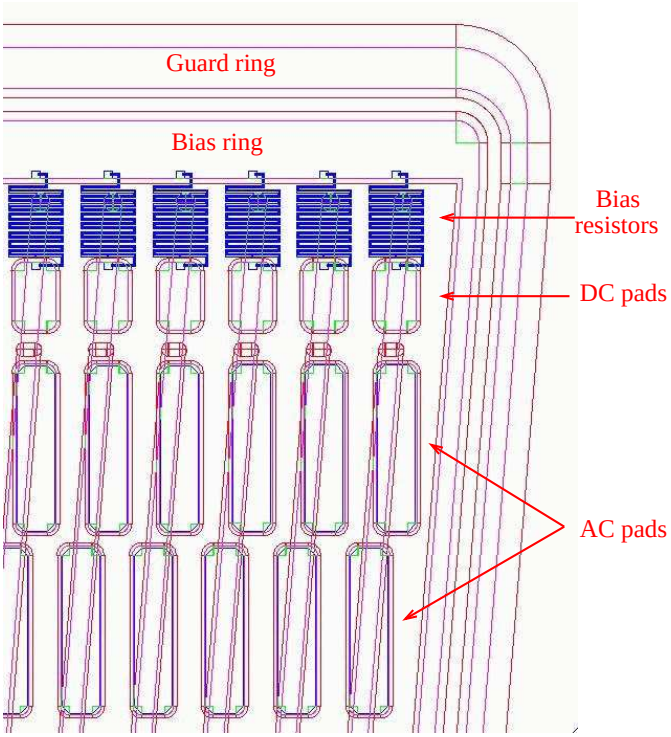

Figure 2: View of one edge of the active region in the W3 detector.

marks is drawn as an opening in the metal layer over the n^+ implanted region, for assembling and mechanical survey purposes. Each sensor is identified by a binary code created by scratching dedicated pads in the non-active region, containing information on the company, the wafer supplier, the sensor type and number. A similar identification scheme is requested in the test-structures area.
Details of the process are under the producer responsibility and hence can vary for thin and thick sensors. However the fabrication process for each of these is kept constant for the whole production.

2 Sensor geometries

The natural coordinate frame used to describe the CMS detector geometry is a right-handed cartesian system with the x axis pointing to the centre of the LHC ring, the z axis coincident with the CMS cylinder axis and the y axis directed upward along the vertical. The cylindrical symmetry of CMS design drives to use a pseudo-angular reference frame given by r, the distance from the z axis, ϕ, the azimuthal coordinate with respect to the x axis, and η, the pseudo-rapidity.

The SST instruments the area from 20 to 120 cm in r and from 0 to 280 cm in $|z|$, with a pseudo-rapidity coverage up to 2.5. The SST can be subdivided into quarters; a longitudinal cut out of one quarter is shown in Fig. 3 [1] [2]. The inner barrel (TIB) has four layers, the outer barrel (TOB) has six layers. The inner end-cap (TID) is made of three small disks on each side of the inner barrel. The outer end-cap (TEC) is made of nine big disks on both sides of the Tracker.

The CMS tracker sensors are foreseen in 15 different geometries: two rectangular detectors for the TIB (Tab.1),

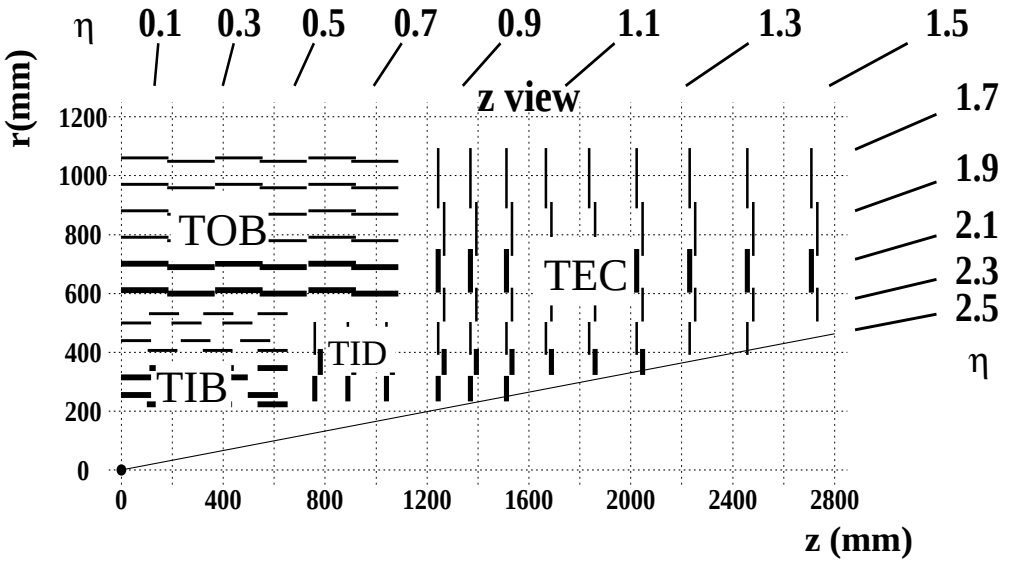

Figure 3: Sketch of the tracker layout (1/4 of the $r-z$ view). Thin lines represent single modules, thick lines double module.

two for the TOB (Tab.1), eleven wedge-shaped detectors for the TID and the TEC (Tab.2). Each detection unit in the inner region (TIB, TID and the first four ring of TEC) is composed by a single micro-strip thin sensor and by two daisy-chained thick sensors in the outer region (TOB and the last three rings of TEC). The first two layers in TIB and TOB, the first two rings in TID and rings 1,2, 5 in TEC are instrumented with double-sided modules. These are made of two independent single-sided detection units, mounted back to back, with the second one being rotated of 100 mrad with respect to the first.

All over the Tracker the strip pitch varies from the inner to the outer layers (from 80 μm to 205 μm). The number of strips is tuned in order to match the electronics modularity of 256 channels. The choice of the range for the strip pitches is also driven by two particle separation capability and by the achievable two-hit resolution, whereas the range of strip lengths minimizes occupancy and noise levels.

In the barrel part rectangular sensors have the strips parallel to the beam to provide the $r-\phi$ information.

The wedge detectors measure the ϕ coordinate and are designed, ring by ring, with the strips pointing to the beam axis. This results in a constant angular pitch in each ring and consequently in a linear pitch that varies slightly in the direction orthogonal to the strips.

Table 1: Inner Barrel (IB) thin sensors and Outer Barrel (OB) thick sensors. The active region is defined as the area inside the bias ring. The physical region is delimited by the cutting line. L refers to the shorter side of the detector and H to the longer one. Quantities do not take into account the spare sensors.

Type	L active/physical [mm]	H active/physical [mm]	Pitch [μm]	Strips	Quantity
IB1	61.5 /63.3	116.9 /119.0	80	768	1536
IB2	61.5 /63.3	116.9 /119.0	120	512	1188
OB1	93.9/96.4	91.6/94.4	122	768	3360
OB2	93.9/96.4	91.6/94.4	183	512	7056

Table 2: Thin (W1-W4) and thick (W5a-W7b) wedge sensors for TID and TEC: W1 has two different versions for TID and TEC, whereas the TID shares identical W2 and W3 sensors with the TEC. The active region is defined as the area inside the bias ring. The physical region is delimited by the cutting line. L1 and L2 are the parallel sides of the detector, H is the height. Quantities do not take into account the spare sensors. The linear pitch for the wedge detectors is defined as the average on all the strips. The two pitch values in the table refer to the shorter and longer side respectively.

Type	L1 active/physical [mm]	L2 active/physical [mm]	H active/physical [mm]	Pitch [μm]	Strips	Quantity
W1 TEC	63.1 /64.6	85.8/87.9	85.2/87.2	81/112	768	288
W1 TID	62.1 /63.6	91.7/93.8	110.9/112.9	80.5/119	768	288
W2	86.6 /112.2	110.1/112.2	88.2/90.2	113/143	768	864
W3	63.3 /64.9	81.1/83.0	110.7/112.7	123/158	512	880
W4	58.1/59.7	71.3/73.2	115.2/117.2	113/139	512	1008
W5a	96.5/98.9	109.5 /112.3	81.2/84.0	126/142	768	1440
W5b	110.0/112.5	120.1/122.8	63.2/66.0	143/156	768	1440
W6a	83.6/86.1	94.6/97.4	96.1/99.0	163/185	512	1008
W6b	94.5/97.5	104.7/107.5	84.9/87.8	185/205	512	1008
W7a	71.5/74.0	80.1/82.9	106.9/109.8	140/156	512	1440
W7b	80.4/82.9	88.0/90.8	94.9/90.8	156/172	512	1440

3 Test structures

The wafer hosts additional devices around the main detector, designed to monitor the stability of the fabrication process. A set of nine structures (standard half-moon) is placed inside a fiducial region as shown in Fig.4. The design is identical for the two suppliers. From left to right it is composed by:

- The "Test Structure for Capacitor" (Ts-Cap) is an array of 26 AC coupled strips, with a pitch of 122 μm, characterized by the same dielectric composition of the main sensor but with a direct connection to the bias ring, without poly-silicon resistors. Each strip, 30 μm large and 4413 μm long, can be read from an AC pad that is placed alternatively on the two opposite sides. This device is used to analyse the quality of the dielectric, measuring its breakdown voltage and the capacitance value.

- The "Sheet" is composed by nine superficial structures, to measure sheet resistance: three implant strips, three aluminum strips, three poly-silicon resistors, all lying directly on the n-doped bulk. All the nine structures have a separate contact on one side of the device, whereas on the opposite end of the strip or of the resistor they are connected to a common bias ring.
  The three poly-silicon resistors are equal to the ones designed to bias the strips on the main sensor. The resistivity of the aluminum and of the p^+ implant is estimated with two sets of three strips, of different width and approximately of the same length (Tab.3). Assuming a constant depth of the implant, the sheet resistivity can be defined dividing the total resistance value by the number of squares in which the area of each structure can be decomposed.

Table 3: Dimensions (in microns) of the aluminum and of the p^+ implanted strips in the Sheet structures.

	HPK	STM
width p^+ strip N.1	12	10
number of square p^+ strip N.1	727	872
width p^+ strip N.2	22	20
number of square p^+ strip N.2	399	438
width p^+ strip N.3	52	50
number of square p^+ strip N.3	172	179
width Al strip N.1	8	8
number of square Al strip N.1	1087	1087
width Al strip N.2	18	18
number of square Al strip N.2	486	486
width Al strip N.3	48	48
number of square Al strip N.3	185	185

- The following structure hosts four Gate Controlled Diodes (GCD), two circular ones on the upper side and two square ones in the lower side. In the square geometry, one of the GCDs is composed by a comb shaped MOS intertwined with a comb made of p+ implanted strips. In the second one the aluminum strips are replaced by poly-silicon implanted strips. The GCDs are used to study the quality of the silicon$-$oxide interface through the measurement of the surface current.

- The "Inter-strip Capacitance AC" (IS-CAP-AC) is a device built of two sets of nine strips with the same structure of the main sensor. In one of them, the poly-silicon resistors are aligned on the same side. The width of the strips is 30 μm, the length 10170 μm and the pitch 122 μm. In the second set the poly-silicon resistors are alternatively on the two sides of the device, the strip width is 20 μm and the pitch 83 μm. This structure is aimed to measure the inter-strip capacitance between the central strip in each group of nine, and the two neighboring ones. The three external strips on each side are connected together through their metallization, to simulate the effect on the capacitance of the strips beyond the first neighbors, in order to minimize the number of connections.

- The standard mini-sensor is a small-size replica of the main sensor. It is a rectangular detector, with an active area of 2.3 $\times$ 1.6 cm^2, composed by 192 strips, with a pitch of 120 μm. This value is an average among the pitches of the different sensor geometries characterizing the SST. The dimensions of the bias and of the guard rings, and the openings in the passivation layer vary slightly between thin and thick wafers, according to the sensor design rules chosen by STM and HPK. On the side of the poly-silicon resistors, the second row of AC pads is displaced by 2 mm with respect to bias ring, in order to perform bonding tests.

The mini-sensor can be used to perform the same measurements that can be done on the main sensor. Moreover it is used to check the required radiation hardness.

- The "Inter-strip Capacitance DC" (IS-CAP-DC) has a similar structure to IS-CAP-AC but the strips are not connected to the bias ring, either directly or through a bias resistor. In addition the capacitor dielectric layer is missing in the strips and the p^+ implant can be contacted all over their length. IS-CAP-DC has been designed to measure the inter-strip resistance.
- A simple square diode, of area 0.24 cm^2, surrounded by a guard ring, is included in the standard half-moon. It is designed to measure the depletion voltage.
- Two Mos devices with a gate area of 0.24 cm^2 each are included in the standard half-moon. MOS1 and MOS2, in the HPK structures and MOS1 in STM wafers have a dielectric composition corresponding to the thick oxide layer present in the inter-strip region of the main detector. In the STM MOS2 the dielectric layer follows the structure of the capacitor in the detector strips. It is hence made of thin layers of SiO_2 and Si_3N_4. These devices are designed to measure the oxide thickness and the flat band voltage value.

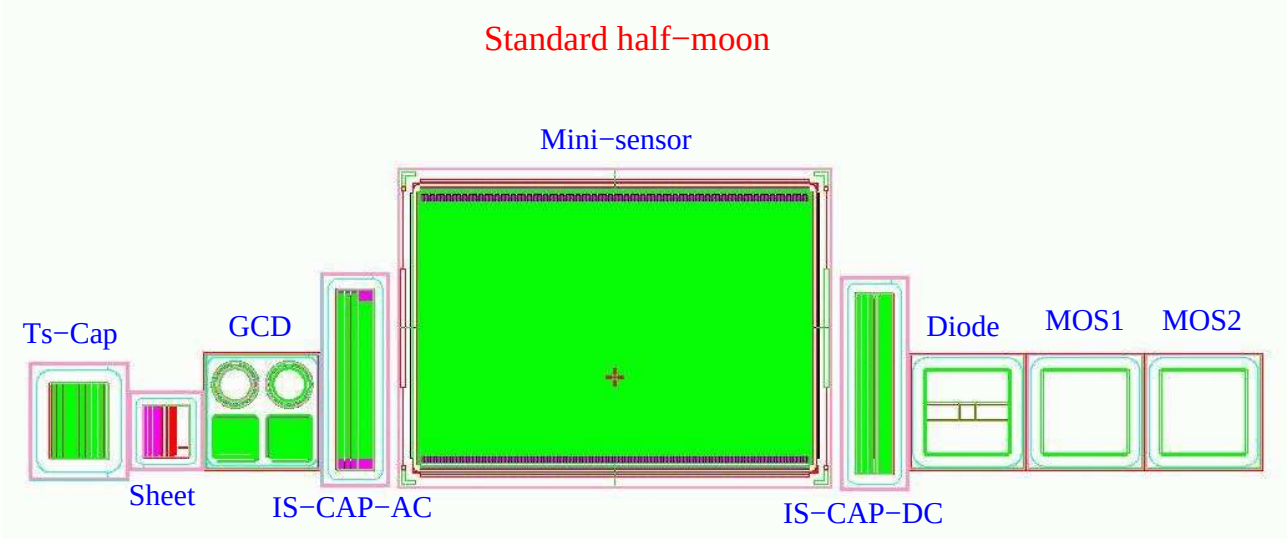

Figure 4: View of the set of nine test structures called "standard half-moon"

An additional mini-sensor is present in each wafer. It is designed with the same pitch and pad arrangement of the main detector on the read-out side, to be used for tests with the read-out electronics. It is characterized by a reduced length and a smaller number of strips with respect to the main sensor, depending on the available space left on the wafer.

4 HPK Silicon Sensors

4.1 Wafer layout

HPK sensors are placed in the wafer inside a fiducial region, shaped as a circle of 139480 μm diameter (Fig. 5 as an example). Additional structures are present along the four sides of the main sensor: the standard half moon (described in Section 3), Mos devices and diodes to check for the quality of the substrate and of the oxide layer, the mini-sensor.

4.2 Strip structure

The widths of the p^+ and metal layer of the strips in all the sensor types follow the rules described in Section 1. The metal over-hang is 6 μm in the DC pads and 5 μm in the AC pads. The openings in the passivation layer on the DC and AC pads are inside the region defined by the implant layer, as requested by the producer. These apertures define the available space for testing and bonding on the pads. The AC pads have an additional layer of poly-silicon, covering the not passivated region, underneath the metal layer. The strips have rounded borders both in the implant and in the metal layer. The distance between the end of the strips and the bias ring, on the sides

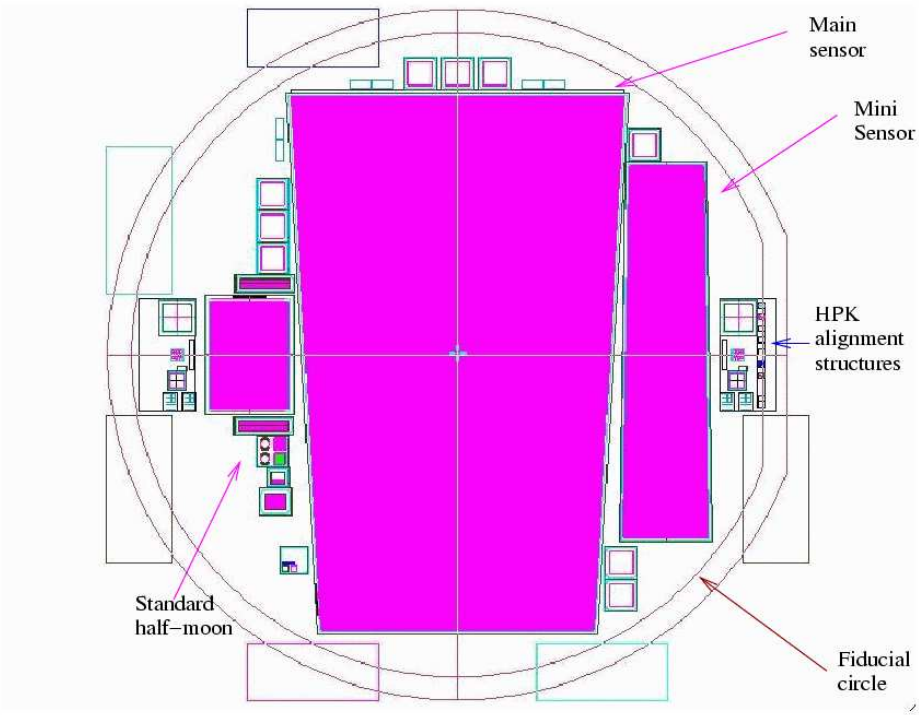

Figure 5: Layout of the HPK wafer for the W4 detector

perpendicular to the strip direction, is 30 μm in the implant layer. The distance between the external strips and the bias ring on the side along the strip direction, depends on the sensor type. The poly-silicon bias resistor is produced above the corresponding strip implant. The bias resistors are always aligned on the same side and they follow two basic designs: R_1, implemented in the W3 sensor, and R_2, for all the other detectors (Tab. 4). The mini-sensor included in the standard half-moon is designed with the bias resistor of the R_2 type, since this is the most common design among the HPK detectors.

Table 4: Characteristics of the two bias resistor types present in the HPK sensors.

Resistor type	Length [μm]	Width [μm]	Number of squares
R_1	200	120	413
R_2	400	70	422

4.3 Bias and Guard ring

The structure and the width of the bias and guard ring are the same for all the sensors provided by HPK. Dimensions are summarized in Tab. 5. The openings in the passivation layer on the bias ring run for all the length of the sides perpendicular to the strip direction and they cover the length of the pads on the sides parallel to the strip direction. The guard ring has openings in the passivation layer only in the four corners of its structure (Fig. 6). The bias and the guard rings have rounded corners except for the most internal implant and metal lines, defining the active region.

4.4 Structure of the detector non-sensitive region

The distance between the external edge of the p^+ implant of the guard ring and the internal side of the n^+ zone is 300 μm on all the detector sides. The width of the n^+ region is 450 μm, with a metal over-hang in the internal edge of 50 μm and in-hang of 20 μm in the external edge. The passivation layer is opened along the cut region. The strip numbers and the reference figures for alignment are designed as apertures in the metal layer over the n^+

Table 5: Dimensions (in microns) of the bias and guard rings in the HPK sensors.

		Implant width	Metal over-hang	
			Internal side	External side
Side along the strip	Bias ring	39	8	18
	Guard ring	39	18	48
Side perpendicular the to the strip	Bias ring	130	8	18
	Guard ring	92	18	48

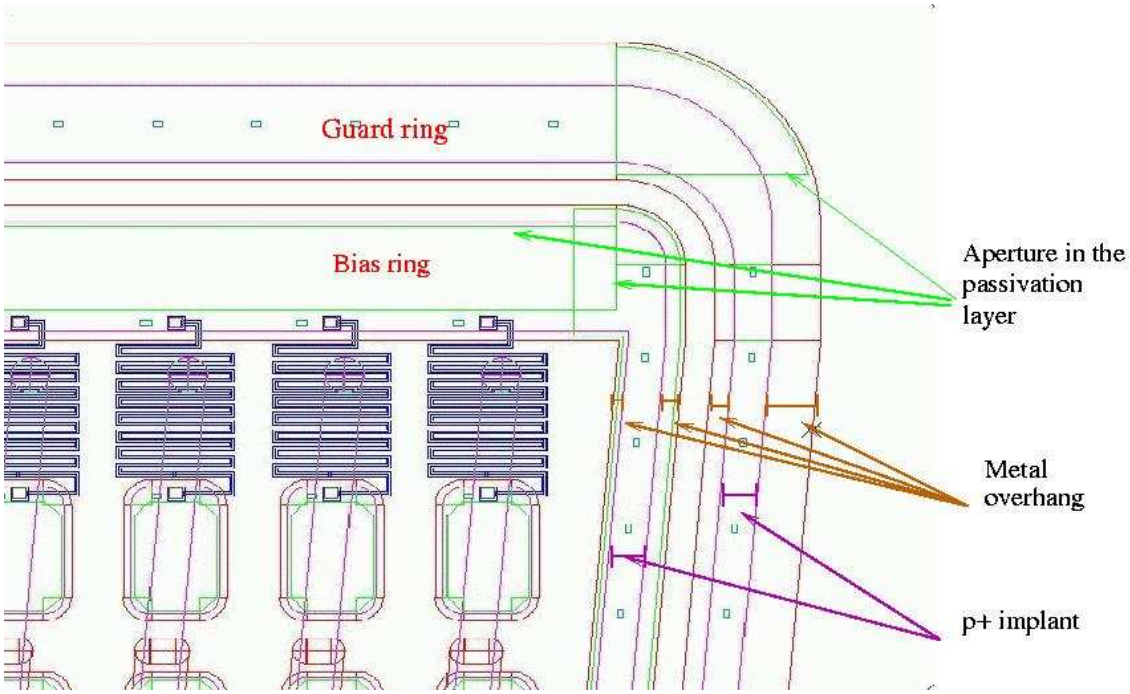

Figure 6: Structure of the bias and guard ring for the HPK sensors. The figure represents one of the edges of the active region in the W3 sensor.

region. The reference figures are L-shaped with a side length of 800 μm for the rectangular sensors (IB1 and IB2) and of 600 μm for the wedge sensors (W1 to W4), as shown in Fig. 7. The numbering scheme is also visible in the figure, and increases from left to right when the side with poly-silicon resistors is on the upper part of the sensor.

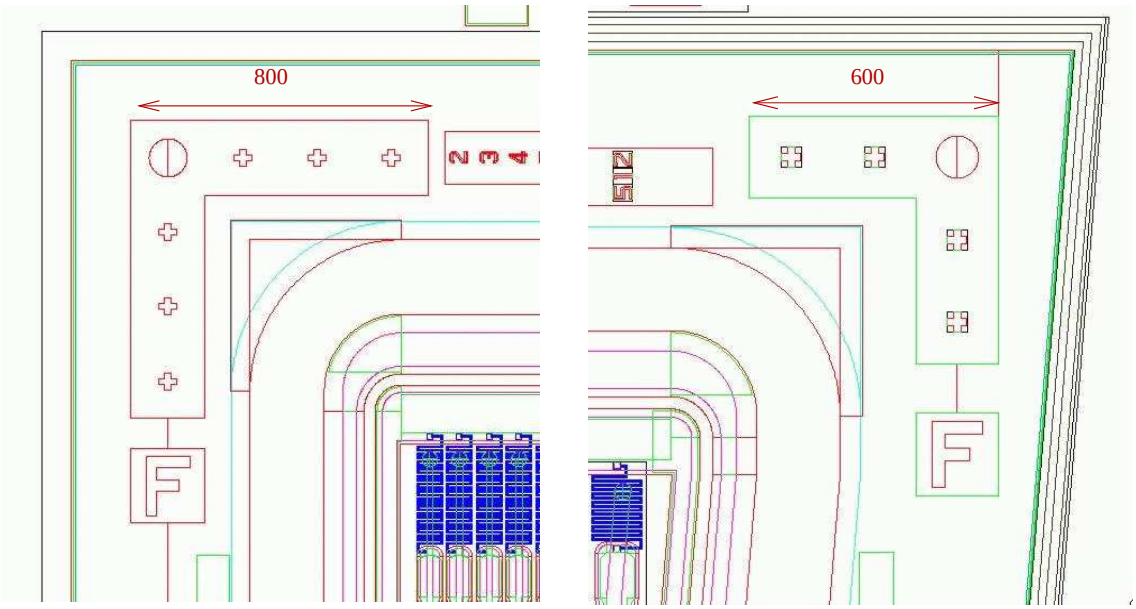

Figure 7: Reference figures, used for alignment: on the left in the case of the IB1 and IB2 detectors, on the right for the wedge sensors. Dimensions are expressed in μm.

4.5 Review of the characteristics of HPK sensor type

The geometrical dimensions of all the sensor types are given in the schematics of the mask designs included in this note (Fig. 26-40). Only the peculiarities of each detector design are illustrated in the following.

4.5.1 IB1

IB1 is a rectangular detector designed with 768 strips at a pitch of 80 μm, the narrowest one among all the 15 different geometries of the CMS silicon sensors. The detector will be mounted on 768 double-sided modules in the two inner layers of the TIB. The conventional read-out side is the one opposite to the bias resistors.
The width of the implant strip is 20 μm, and the width of the strip metallization 28 μm. The choice to align all the bias resistors on the same side has led to the need of decreasing the width of the DC pads with respect to the other sensor types (the opening in the passivation layer is 62 μm large). The AC pads are staggered in two different rows for adjacent strips, allowing to keep the pads large enough for bonding purposes. In this way the total number of AC pad rows on either side of this sensor sums to 4. The arrangement of the pads on the strips is shown in Fig. 8.
The relevant dimensions of the IB1 sensor are reported in Tab.1 and in Fig.26.
The IB1 mini-sensor is designed with 128 strips and the active region measures $10320 \times 80000\ \mu m^2$.

4.5.2 IB2

IB2 has identical external dimensions with respect to IB1 but only 512 strips, resulting in a pitch of 120 μm. This detector will be mounted on 1188 single modules in the two outer layers of the TIB. The conventional read-out side is the one opposite to the bias resistors.
The width of the implant strip is 30 μm, and the width of the strip metallization 40 μm. The wider space available between strips has allowed to keep both DC and AC pads at the same level for adjacent strips, resulting in one DC pad row and two AC pad rows on either side of the detector (Fig.9).
Dimensions of the IB2 sensor are listed in Tab.1 and Fig.27.
The IB2 mini-sensor has 64 strips and the active region is $7720 \times 50000\ \mu m^2$.

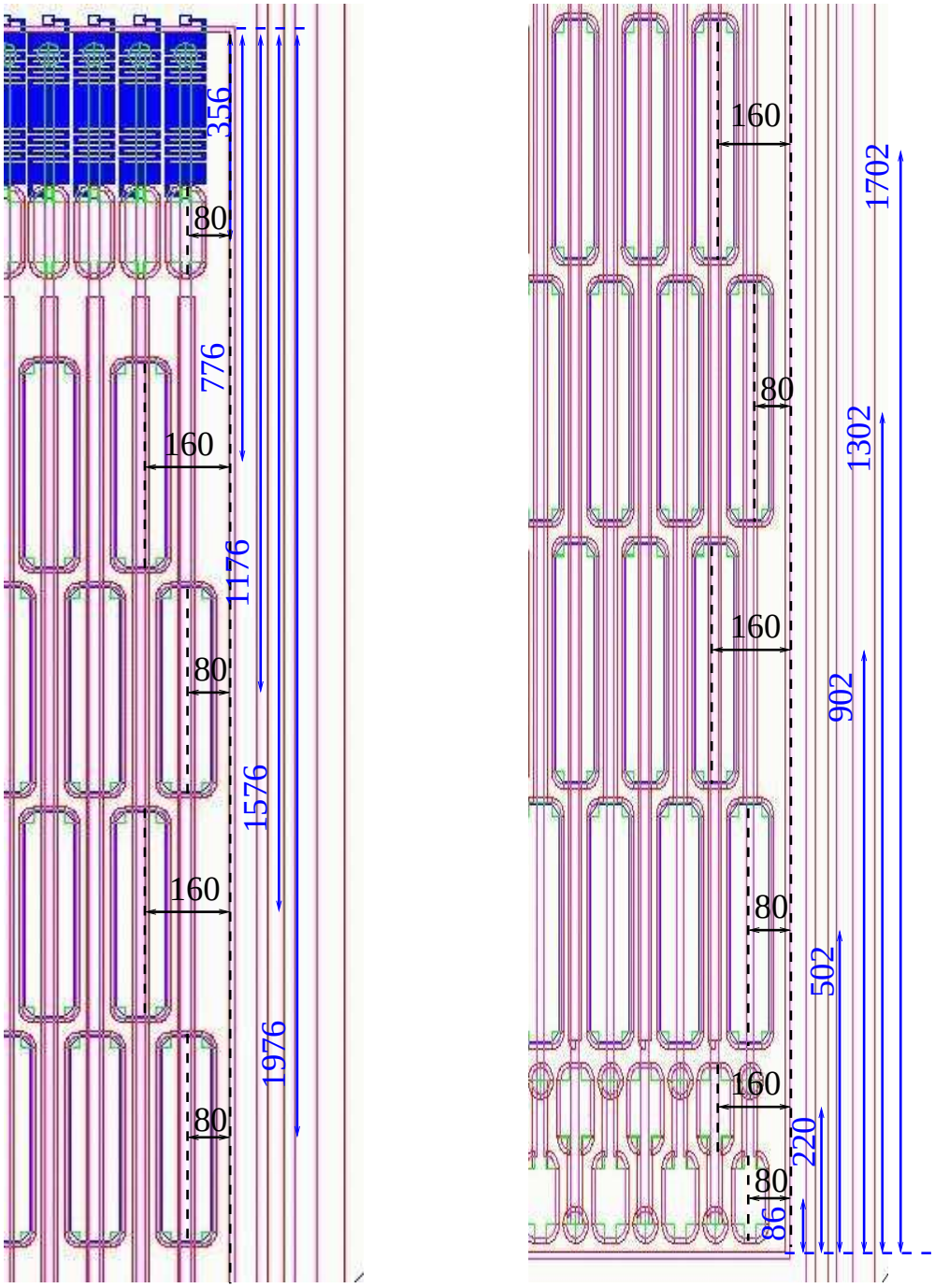

Figure 8: Views of the edges of the active region on the two opposite sides of the IB1 detector. Distances are expressed in μm.

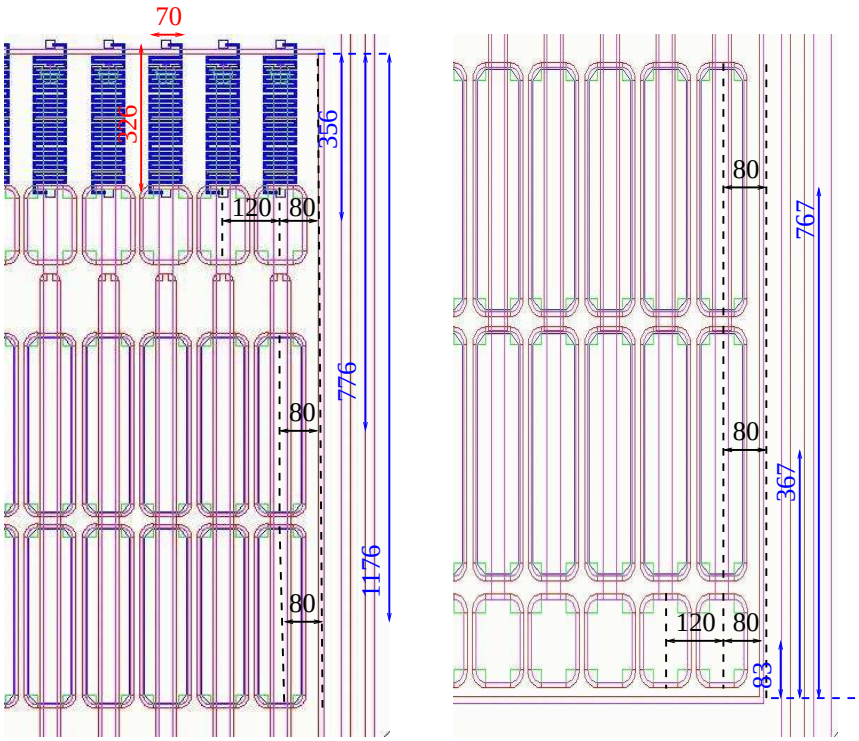

Figure 9: Views of the edges of the active region on the two opposite sides of the IB2 detector. Distances are expressed in μm.

4.5.3 W1 TEC and W1 TID

The first rings of the TEC and of the TID use wedge detectors with the same angular pitch (0.019852°), but of different length. The TID sensor has been designed 25700 μm longer and at a lower inner radius (231300 μm instead of 235100 μm for W1 TEC, measured at the internal edge of the bias ring) to cover regions where the SST would otherwise have no acceptance. The W1 detectors will be mounted on 144 double-sided modules, both in the TEC and in the TID, with 24 modules in ϕ in each of the 6 disks. The conventional read-out side is the longer base, where the poly-silicon resistors have been designed.
In both the W1 detectors was impossible to arrange the DC and AC pads at a constant step all along the detector width, since the linear pitch varies largely between the external and the internal strips. For example, in W1 TEC, the pitch between the most external strips is 112.8 μm, whereas between the two central strip is 111.0 μm. In order to keep the possibility of testing the sensor with a probe-card, we have chosen to build a group of pads, inside which the step is constant. This group is repeated all along the detector width, but the position of the first pad in the group is adjusted in such a way that all the pads contact the corresponding strips. So the pad step is constant everywhere except between the $(N \times i)$th and $(N \times i + 1)$th pads, where N is the number of pads in the group and i is the group repetition index. In W1 TEC and W1 TID each group is made of 16 pads on the wedge wider base and 8 pads on the narrower one. Here the pad distance corresponds to twice the strip pitch, since the even and odd DC and AC pads are staggered in two different rows (Fig.10 and Fig.11).
In W1 TEC the implant (metal) layer of the strip is 28 (36) μm large on the bias resistor side, and 20 (28) μm on the opposite side. In W1 TID the strip width varies between 20 (28) and 30 (40) μm in the implant (metal) layer. Dimensions of the W1 TEC and W1 TID sensors are listed in Tab.2 and Fig.30, Fig.31.
The W1 TEC mini-sensor has 128 strips, an active length of 80000 μm, and the two opposite sides of the active region measure 10754 and 14272 μm. The active region of the W1 TID mini-sensor is 80000 μm long, the two basis measure 5944 and 7690 μm and the number of strips is 64.

4.5.4 W2

The W2 detector is the active element of the second ring in the TEC (288 double-sided modules) and of the TID (144 double-sided modules, 24 modules in ϕ for each disk). W2 will be read out by the longer base, the poly-

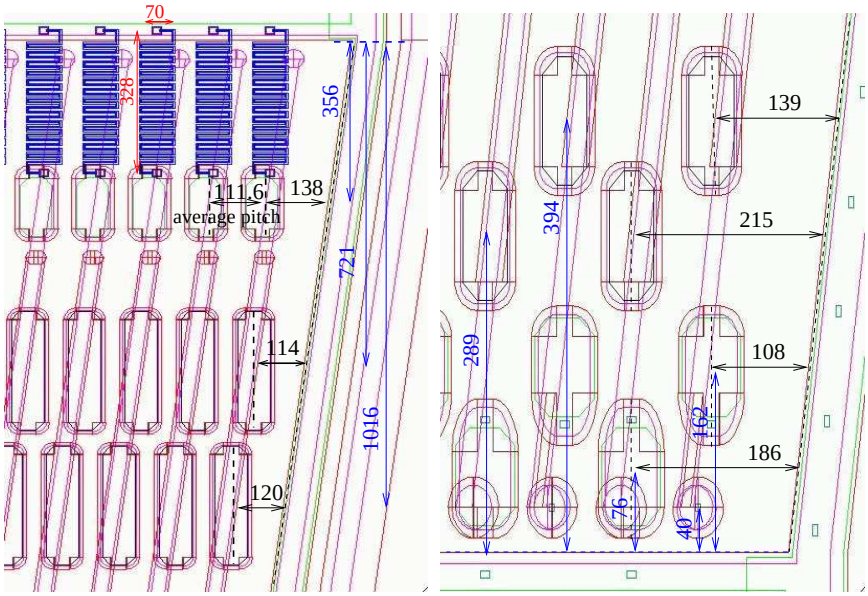

Figure 10: Views of the edges of the active region on the two opposite sides of the W1 TEC detector. Distances are expressed in μm.

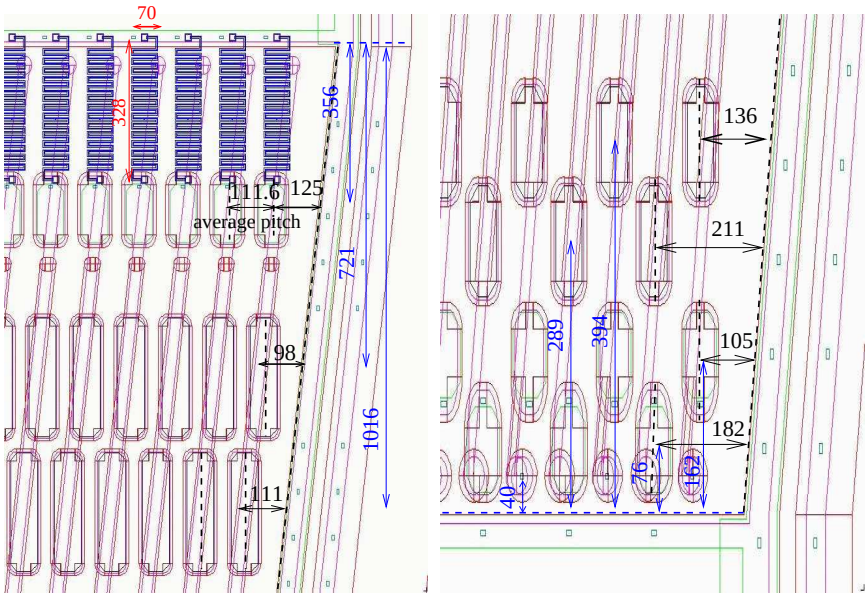

Figure 11: Views of the edges of the active region on the two opposite sides of the W1 TID detector. Distances are expressed in μm.

silicon resistor side. The inner radius of the active region is 323000 μm, and the angular pitch 0.01985 °.
Also in this case it was not possible to keep a constant step among all the pads and a similar arrangement to the W1 one has been adopted. On both the sensors bases the pad groups are composed of 16 elements. The DC pads and the first row of AC pads are aligned along the vertical axis (Fig.12). In W2 the strip width goes from 28 (36) to 36 (46) in the implant (metal) layer.
Dimensions of the W2 sensor are listed in Tab.2 and Fig.32.
The W2 mini-sensor has 64 strips, and the active region is 45000 μm long, with the two basis measuring 8190 and 9172 μm.

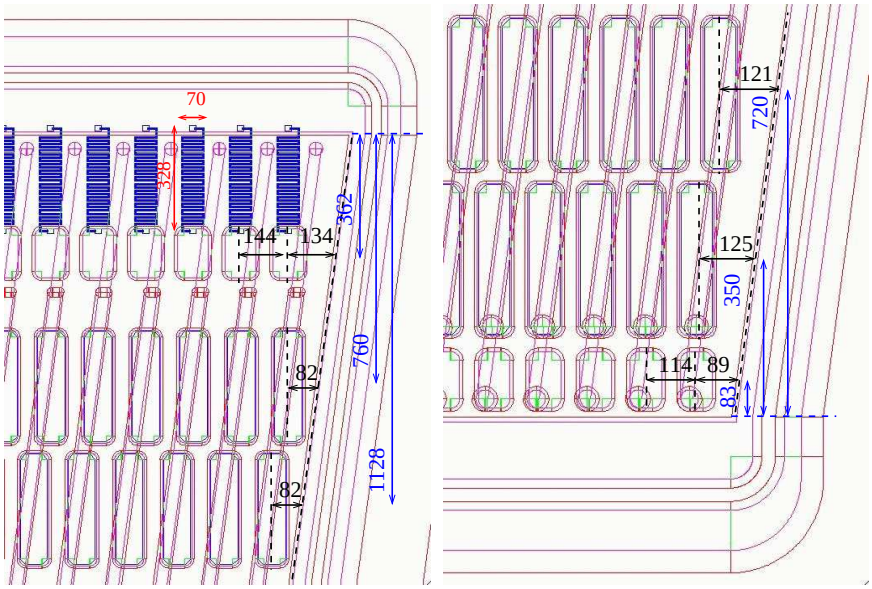

Figure 12: Views of the edges of the active region on the two opposite sides of the W2 detector. Distances are expressed in μm.

4.5.5 W3

This wedge detector, made of 512 strips, is the sensitive element of the third ring in the TEC (640 single modules, 40 modules in ϕ in each disk) where it is read from the bias resistor side, and of the third ring in the TID (240 single modules) where it is read from the opposite side.
The angular pitch is 0.01799° and the inner radius of the active region is 392100 μm.
On the implant (metal) layer, the strip is large 31 (41) μm on the bias resistor side and 39 (51) μm on the opposite side. Only in this sensor, among the ones produced by HPK, the insertion of the shorter resistor type (R_1) was possible, due to the larger linear pitch of the strips.
DC and AC pads on both sides are positioned at a constant step along all the sensor width, as shown on Fig.13. On the top side, the DC pads and the first row of AC pads are exactly aligned on the vertical axis to allow an easier testing procedure. All the strips are numbered on both sides.
Dimensions of the W3 sensor are listed in Tab.2 and Fig.33.
The W3 mini-sensor has 64 strips, the active region is 50000 μm long and the two basis measure 9130 and 10118 μm.

4.5.6 W4

This wedge detector, made of 512 strips, is the sensitive element of the fourth ring in the TEC (1008 single modules, 56 modules in ϕ in each disk) where it is read from the bias resistor side.
The inner radius of the active region is at 504100 μm and the angular pitch is 0.012856°.
On the implant (metal) layer, the strip is large 35 (45) μm on the bias resistor side and 28 (36) μm on the opposite side.
DC and AC pads are positioned following the same criteria as in the W3 detector (Fig.14). Dimensions of the W4 sensor are listed in Tab.2 and Fig.34.

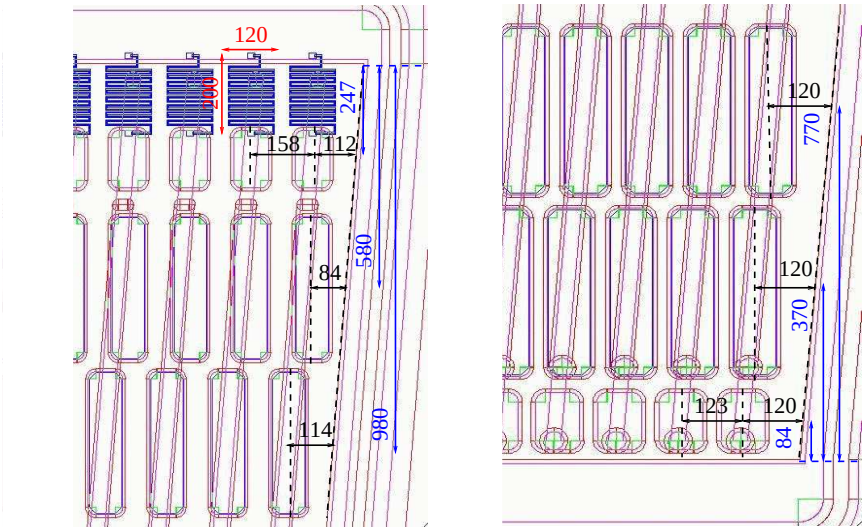

Figure 13: Views of the edges of the active region on the two opposite sides of the W3 detector. Distances are expressed in μm.

The W4 mini-sensor has 128 strips, the active length is 80000 μm and the basis dimensions are 15548 and 17826 μm.

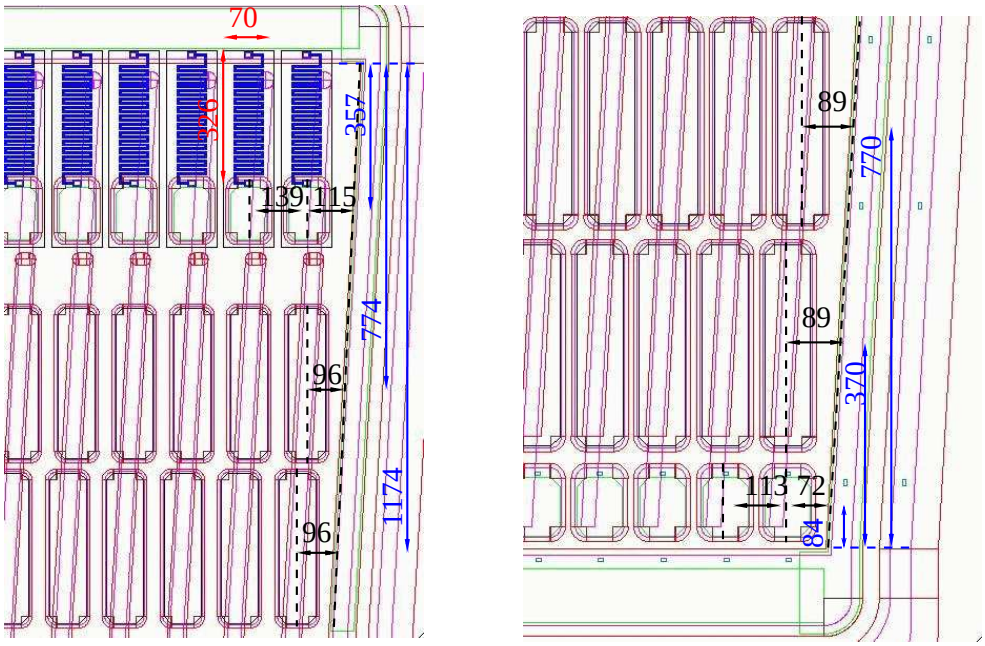

Figure 14: Views of the edges of the active region on the two opposite sides of the W4 detector. Distances are expressed in μm.

5 STM Silicon Sensors

5.1 Wafer layout

Thick sensors foreseen for the CMS silicon tracker are produced by STM. Each wafer contains a large area sensor located inside a circular region of 139480 μm diameter, where the process quality is guaranteed.
The available space surrounding the main sensors houses additional structures: the standard half-moon, MOS devices and diodes, a mini-sensor and some specific structures required by the company for the process qualification. The typical layout of a wafer is shown in figure 15.

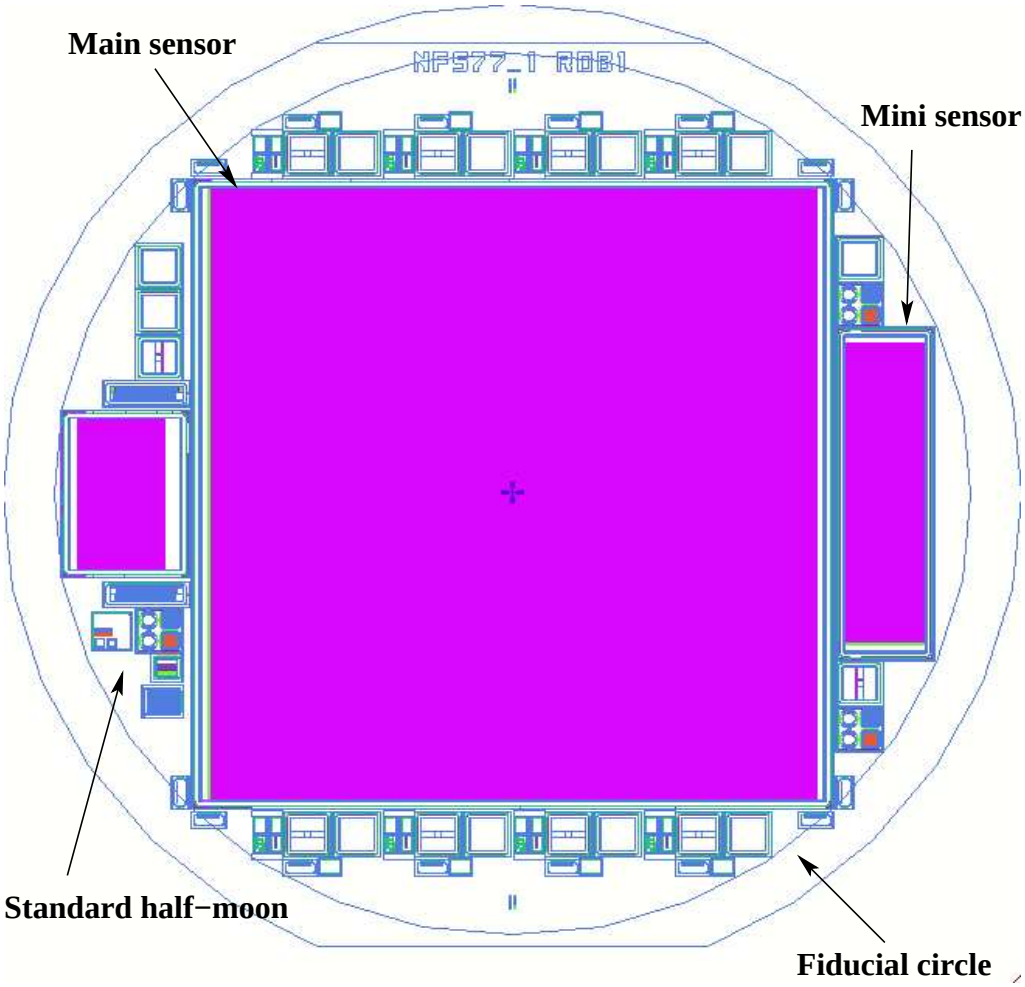

Figure 15: Mask design for the Outer Barrel (OB1) sensors.

5.2 Strip structure

The p^+ implant and the metal layer of the strips are designed following the rules described in section 1.
The strips are biased using poly-silicon resistors aligned on one side. A single design is used for all STM sensor types: each resistor is 100 μm wide, 407 μm long and consists of 665 poly-silicon squares.
One row of DC pads and two rows of AC pads are present on each detector side and are aligned orthogonally to the strip direction. A common feature for the pad design is the use of 6 μm metal over-hang and a contactable region 1 μm wider than the p^+ implant.
The width of the pads is designed as large as possible accordingly with the strip pitch. As a consequence, the dimensions of the pads depend on the sensor design. The values chosen for each detector type are indicated in the sketches included in this note. The optimization of the AC pad design includes the use of a thicker oxide layer under the pad to reduce the probability of damaging the capacitor during the testing and the bonding.
The DC pads are designed as close as possible to the bias ring. The distance between the p^+ implant of the DC pad and the bias ring in the side perpendicular to the strip direction is 433 μm where poly-silicon resistors are designed and 29 μm in the other side. The distance between the first and last strip and the bias ring on the side along the strip direction depends on the sensor type and ranges from 71 to 155 μm.
The distance between the DC and the first AC pads, along the strip, is 20 μm and the second AC pad is designed at a distance of 38 μm from the first AC pad.

5.3 Bias and Guard ring

All the sensors produced by STM have the same bias and guard ring structure, as shown in fig. 16. Each ring is

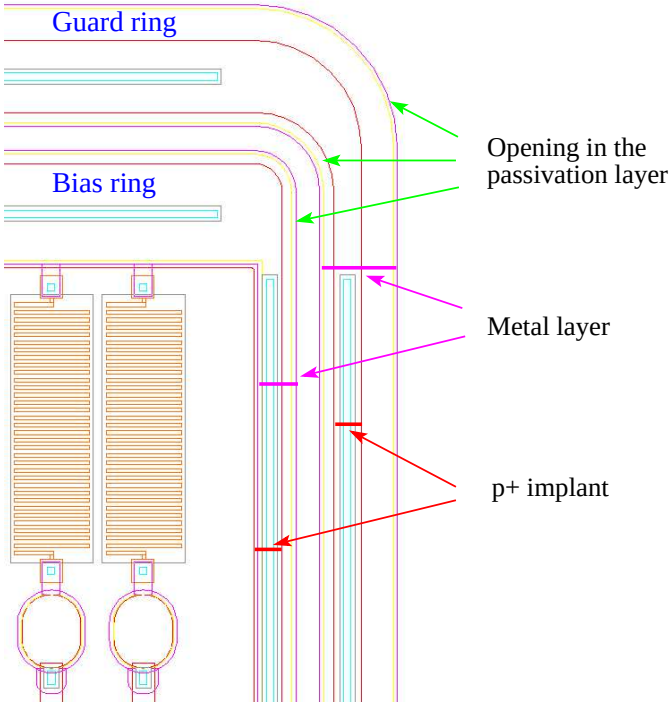

Figure 16: Structure of bias and guard ring for sensors produced by STM.

metallized with an aluminum deposition. The bias ring has a metal over-hang only in the external side and 5 μm metal in-hang in the internal side. On the contrary, a metal deposition wider than the p^+ implant is designed on both sides of the guard ring.
The passivation layer is opened on the larger side of both rings and along the side parallel to the strip direction up to the second row of AC pads.
A detailed description of the geometry for bias and guard ring is reported in Table 6.

Table 6: Dimensions (in microns) of the bias and guard rings in the STM sensors.

		Implant width	Metal over-hang	
			Internal side	External side
Side along the strip	Bias ring	37	-5	18
	Guard ring	37	18	48
Side perpendicular the to the strip	Bias ring	138	-5	18
	Guard ring	96	18	48

5.4 Structure of the detector non-sensitive region

The design of the edge region is the same for all STM sensors type. A schematic view is shown in figure 17.
The n^+ implant is designed at a distance of 700 μm from the external edge of the p^+ implant of the guard ring. In the internal side of the n^+ implant a 50 μm metal over-hang is implemented. The width of the n^+ region is 410 μm for all the rectangular detector sides. In the wedge sensors the n^+ region is 410 μm large in the side perpendicular to the strip direction and has a variable width, not smaller than 410 μm, in the side parallel to the strip direction.
For all the STM sensor type, the distance between the internal edge of p^+ implant of the bias ring and the cutting edge is 1410 μm along the strip direction. The same distance measured orthogonally to the strip direction depends on the sensor design: for rectangular detectors (OB1 and OB2) the value is 1250μm, for the wedge sensors (ring 5, 6 and 7) the range is $1300 \div 1330$ μm.
The identification code is inserted along the strip direction close to the position where poly-silicon resistors are designed.
The strips are numbered on both the sides perpendicular to the strip direction. Numbers are defined using a metal layer over the n^+ implant in a region where the aluminum is not deposited. For each side only even or odd strips are indicated. Strips are numbered from left to right if the side with resistors is in the upper part of the sensor, except for the sensors designed for the seventh ring of the TEC.
The alignment of detectors for module construction is allowed by a suitable marker shown in figure 17. Each side of the L-shaped marker is 800 μm long and 200 μm wide. The circle inside the marker has a diameter of 100 μm and each cross reference is 47 μm long and 15 μm wide. The circular marker has been designed at 260 μm from the external edge of the metal layer. The position and the shape of the marker are equal for all sensors mask layout designed by STM.
The sensors will be diced by the company with a tolerance of $\pm 20 \mu$m. In order to improve the precision of the dicing a square marker has been designed in the detector corners. The marker, shown in the figure, is clearly visible with a microscope and allows to define in a precise way the edge of the cutting line.

5.5 Review of the characteristics of STM sensor types

Eigth different designs are used for thick sensors: two for the rectangular detectors and six for the wedge ones. Thick modules consist of two sensors having the read-out strips daisy-chained with micro-bonding wires.
Rectangular sensors, designed for the outer barrel module (TOB), have parallel strips with a constant linear pitch. Wedge detectors, designed for the end-cap region of the Tracker (TEC), have radial strips with a constant angular pitch. For the ring 5, 6 and 7 of the TEC, two sensor masks, named A and B, have been designed with the same angular strip pitch. The detector A will be installed at a lower radius. The mini-sensor included in the wafer layout for sensor A and B of each ring is identical. It has been designed with the pad position and strip pitch as the read-out side of the corresponding wedge module.
The pitch for DC and AC pads is chosen as the mean value of the distance between two adjacent strips calculated along the detector active region. DC and AC pads have been aligned along the strip direction wherever it was possible.
A detailed geometrical description of each detector is presented in the sketches at the end of the document. The characteristics of each sensor design are discussed in the following.

5.5.1 OB1

OB1 is the first rectangular detector designed to build the modules for the TOB. It has 768 strips with a pitch of 122 μm. The strip has the p^+ implant 30 μm wide and a metallization layer 40 μm wide. One row of DC pads and two rows of AC pads, aligned along the strip direction, are foreseen on each side of the detector. The pad arrangement is shown in figure 18.
The total number of OB1 sensors is 3360. These detectors are required for 1680 single-sided modules that will be

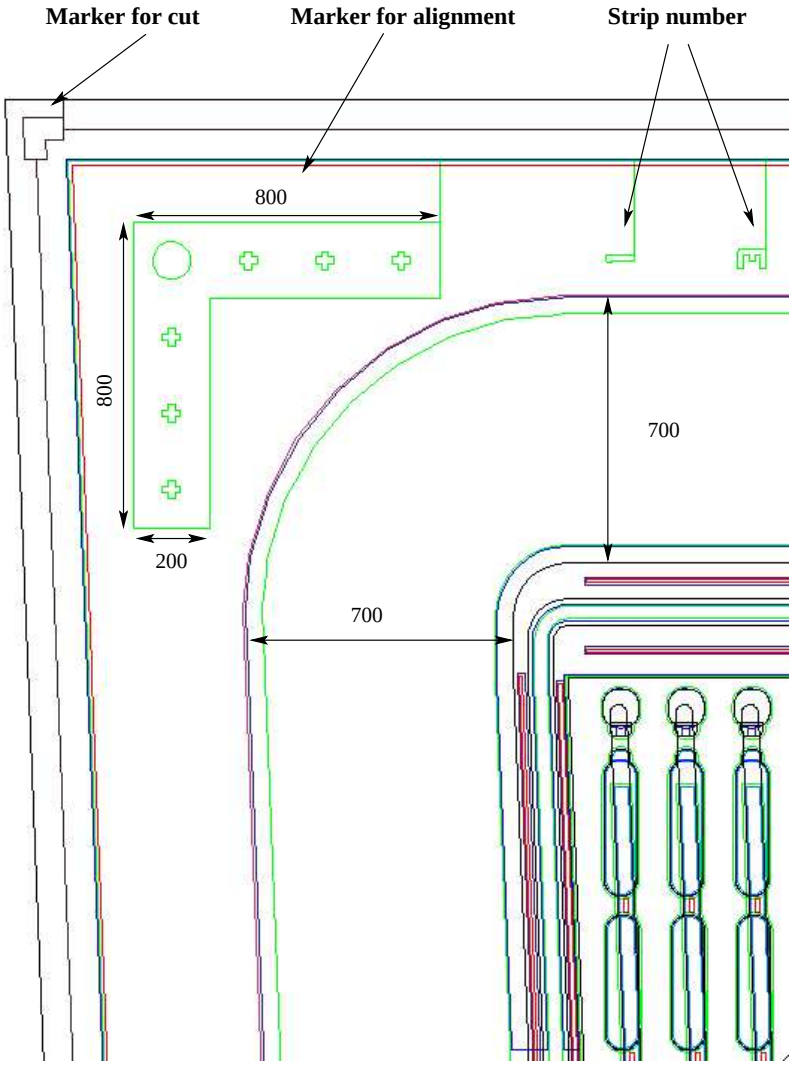

Figure 17: External region of the W7A sensors. Dimensions are expressed in μm.

installed in the layer 5 and 6. The conventional read-out side is the one opposite to the bias resistors.
The dimensions of the OB1 sensors are reported in Tab.**??** and in Fig. 28.
The OB1 mini-sensor has 96 strips and an active area of $11890 \times 50000 \mu m^2$.

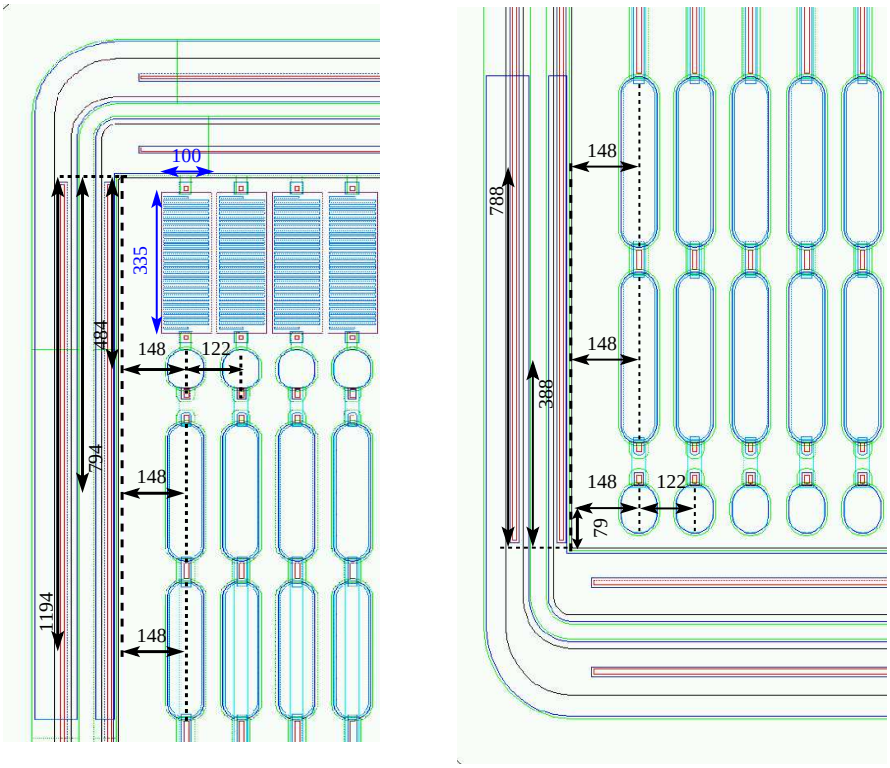

Figure 18: Views of the edges of the active region on the two opposite sides of the OB1 detector. Distances are indicated in μm.

5.5.2 OB2

The second design for outer barrel sensors has the same sensitive area of OB1 detectors, but the number of strips is 512 and the pitch is 183 μm. The p^+ implant of the strip is 46 μm wide and the width of the metal layer is 58 μm. One row of DC pads and two rows of AC pads, aligned along the strip direction, are designed on both sides of the detector, as indicated in figure 19.
These sensors will be used to build 1080 double-sided modules for the first two layers of the TOB and 1368 single-sided modules to equip the third and fourth layers. The conventional read-out side is the one opposite to the bias resistors.
The dimensions of the OB2 sensors are listed in Tab.**??** and in Fig.29.
The OB2 mini-sensor consists of 64 strips and has an active area of $48058 \times 50000 \mu m^2$.

5.5.3 W5 - sensor A

W5A sensors will be used to build 720 double-sided modules for the fifth ring of the TEC. The inner radius of the active area, i.e. the internal edge of the bias ring, is 603200 μm and the angular pitch is $0.011909°$.
W5A detectors have 768 strips with the implant (metal) layer 36 (46) μm large on the resistor side and 31 (41) μm on the opposite side.
One row of DC pads and two rows of AC pads are designed on each side of the detector. Since the linear pitch is varying from the shorter to the larger side of the sensor, along the strip direction the row of DC pads and the first row of AC pads are aligned in the larger side, while a slight misalignment, smaller than 10 μm, is present in the shorter side. The pad arrangement is shown in figure 20.

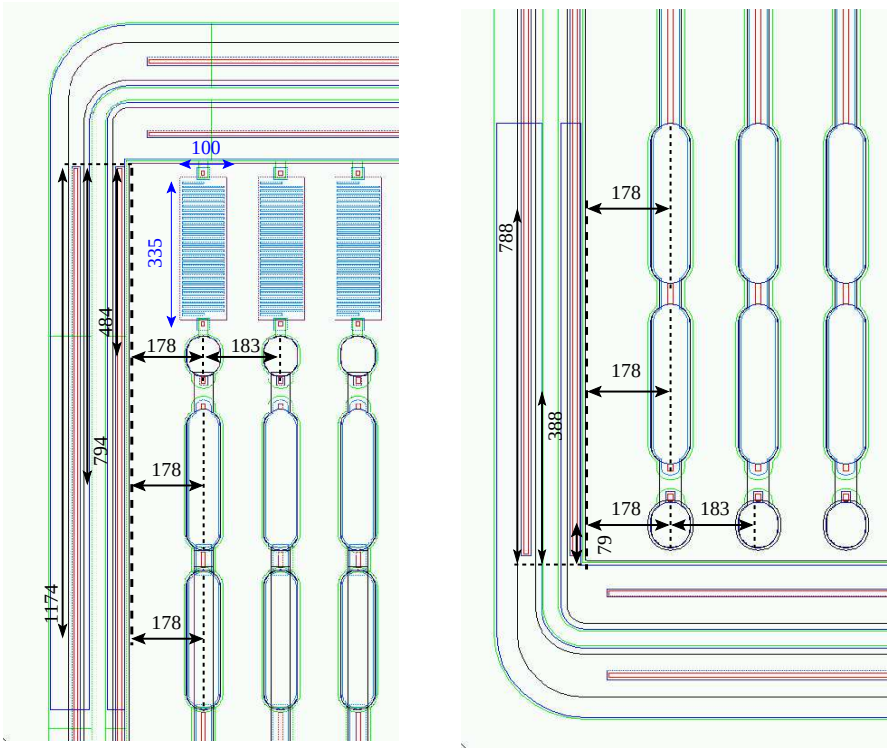

Figure 19: Views of the edges of the active region on the two opposite sides of the OB2 detector. Distances are indicated in μm.

W5A sensors will be assembled with the W5B sensors and the read-out electronics will be placed on the larger side of W5B.
Dimensions of the W5A sensor are reported in Tab.2 and Fig.35.
The W5A mini-sensor has 64 strips with the same pitch of the module read-out side. The active area is 50000 μm long and the two bases are 9332 and 9986 μm^2.

5.5.4 W5 - sensor B

W5B detectors have the same angular pitch as W5A ($0.011909°$) and the inner radius of the active area is 687293 μm.
Detector has 768 strips and the width of the strip implant (metal) layer is 39 (51) on the larger side and 36 (46) μm on the opposite side. One row of DC pads and two rows of AC pads are designed on each side of the sensor. Since the linear pitch is varying from the shorter to the larger side of the sensor, along the strip direction the row of DC pads and the first row of AC pads are aligned in the larger side, while a misalignment, smaller than 18 μm, is present in the shorter side. The pad arrangement is shown in figure 21.
Each sensor will be daisy-chained to a W5A detector and the module will be read-out from the larger side of W5B.
The geometrical details of the W5B sensor are presented in Tab.2 and Fig.36.
The W5B mini-sensor is identical to the one designed in the W5A mask.

5.5.5 W6 - sensor A

W6A sensors will be used to build 1008 single-sided modules for the sixth ring of the TEC.
The angular pitch is $0.012847°$ and the inner radius of the active area is 727000 μm.
The width of the implant (metal) layer of the strip is 46 (60) μm on the larger side and 41 (53) μm on the opposite side.
The strip pitch is large enough to allow for alignment between DC pads and the first row of AC pads. The second row of AC pads is designed with a slightly different pitch, as it is shown in figure 22.
Each sensor will be daisy-chained to a W6B detector and the read-out electronics will be placed on the larger side of W6B.

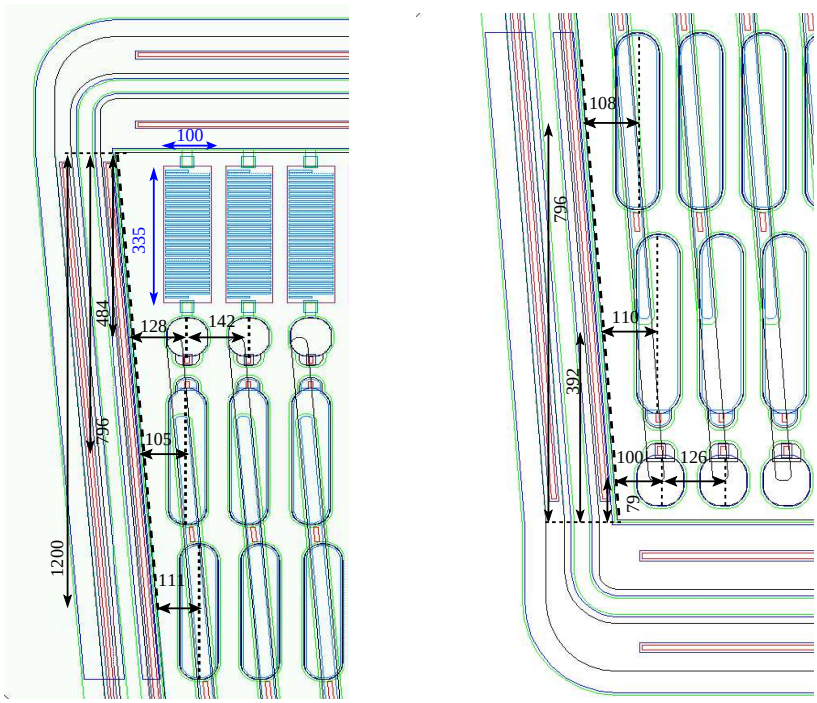

Figure 20: Views of the edges of the active region on the two opposite sides of the W5A detector. Distances are indicated in μm.

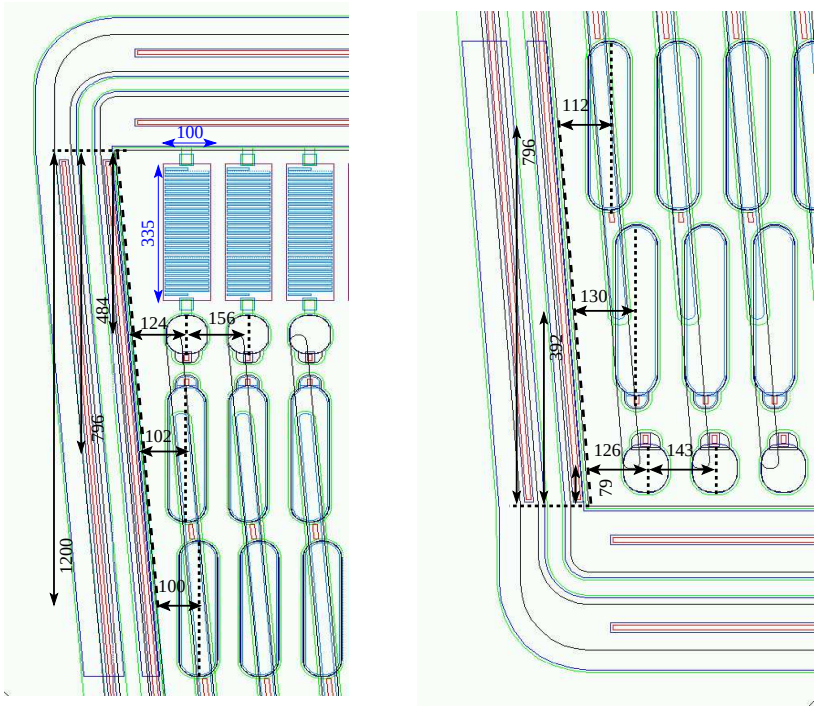

Figure 21: Views of the edges of the active region on the two opposite sides of the W5B detector. Distances are indicated in μm.

Dimensions of the W6A sensor are listed in Tab.2 and Fig.37.
The W6A mini-sensor has 48 strips with the same pitch as the larger side of W6B. The active area is 50000 μm long and the two bases are 9318 and 9890 μm.

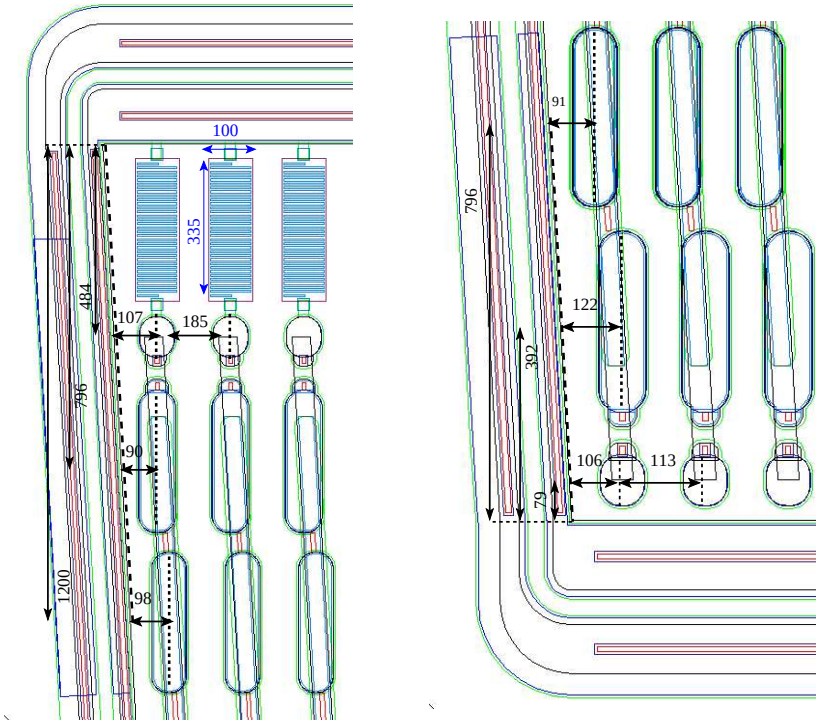

Figure 22: Views of the edges of the active region on the two opposite sides of the W6A detector. Distances are indicated in μm.

5.5.6 W6 - sensor B

W6B sensor has the same angular strip pitch as W6A ($0.012847°$) and the inner radius of the active area is 826060 μm.
The width of the implant (metal) layer of the strip is 51 (67) μm on the larger side and 46 (60) μm on the opposite side.
The strip pitch is large enough to allow for alignment between DC pads and the first row of AC pads. The second row of AC pads is designed with a slightly different pitch, as it is shown in figure 23.
Each sensor will be daisy-chained to a W6A detector and the module will be read-out from the larger side of W6B.
Dimensions of the W6B sensor are listed in Tab.2 and Fig.38.
The W6B mini-sensor is identical to the one designed in the W6A mask.

5.5.7 W7 - sensor A

W7A detectors is designed to build 1440 single-sided modules for the outer ring of the TEC.
The angular strip pitch is $0.009°$ and the inner radius of the active area is 888400 μm.
The width of the implant (metal) layer of the strip is 39 (51) on the larger side and 35 (45) on the opposite side.
The strip pitch is large enough to allow for alignment between DC pads and the first row of AC pads. The second row of AC pads is designed with a slightly different pitch. The pad arrangement is shown in figure 24.
The main sensor has a different scheme for strip numbering. Strips are labeled with numbers growing from left to right when the sensor has the resistor side on the lower part.
W7A sensors will be daisy-chained with the W7B sensors and the read-out electronics will be placed on the smaller side of W7A.
Dimensions of the W7A sensor are listed in Tab.2 and Fig.39.
The mini-sensor has 64 strips with same pitch as the shorter side of W7A. The active area is 50000 μm long and

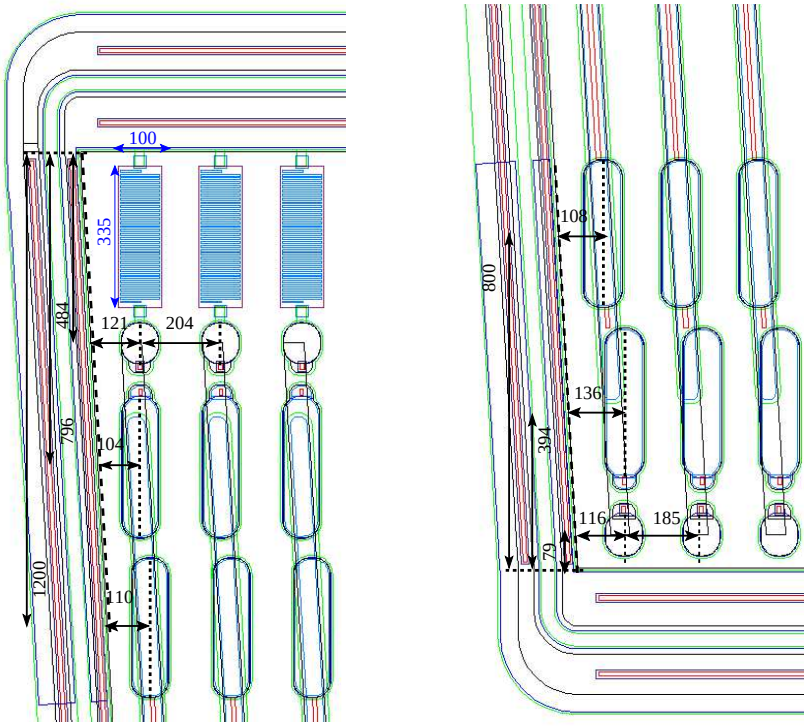

Figure 23: Views of the edges of the active region on the two opposite sides of the W6B detector. Distances are indicated in μm.

the two bases are 8994 and 9486 μm.

5.5.8 W7 - sensor B

W7B detector has the same angular strip pitch as W7A ($0.009°$) and the inner radius of the active area is 998252 μm.
The width of the implant (metal) layer of the strip is 43 (55) μm on the larger side and 39 (51) μm on the opposite side.
The strip pitch is large enough to allow for alignment between rows of DC and AC pads, as it is shown in figure 25.
The strips are numbered as in the W7A sensor.
Each sensor will be daisy-chained to a W7A detector and the module will be read-out from the shorter side of W7A. Dimensions of the W7B sensor are listed in Tab.2 and Fig.40.
The W7B mini-sensor is identical to the one designed in the W7A mask.

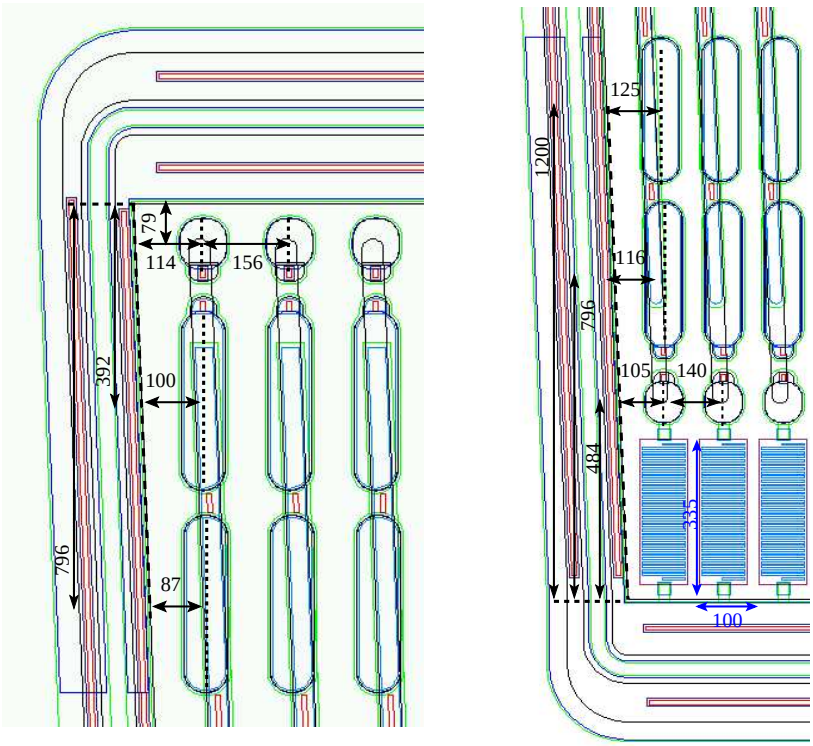

Figure 24: Views of the edges of the active region on the two opposite sides of the W7A detector. Distances are indicated in μm.

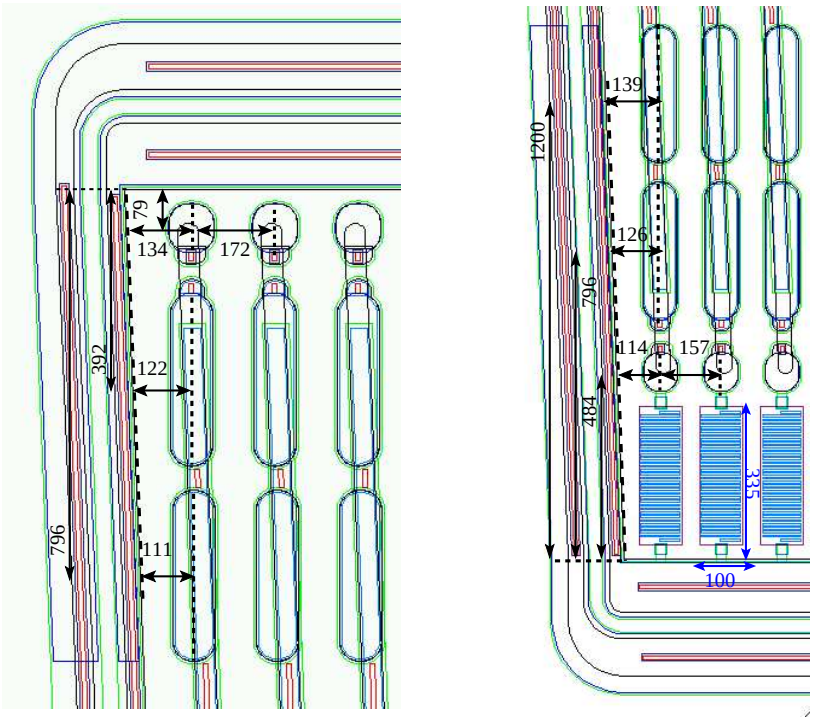

Figure 25: Views of the edges of the active region on the two opposite sides of the W7B detector. Distances are indicated in μm.

References

[1] The CMS Collaboration, “The CMS Tracker Project Technical Design Report”, CMS TDR 5 CERN/LHCC 98-6, 20 April 1998.

[2] The CMS Collaboration, “Addendum to the CMS Tracker Technical Design Report”, CMS TDR 5 CERN/LHCC 2000-16, 21 February 2000.

[3] S. Braibant et al., “Investigation of design parameters for radiation hard silicon microstrip detectors”, Nucl. Instr. and Meth. A 485(2002) 343.

[4] D. Passeri, P. Ciampolini, A. Scorzoni, G.M. Bilei, “Physical modeling of silicon microstrip detectors: influence of the electrode geometry on critical electrical fields”, IEEE Trans. Nucl. Sci. 47 (2000) 1468.

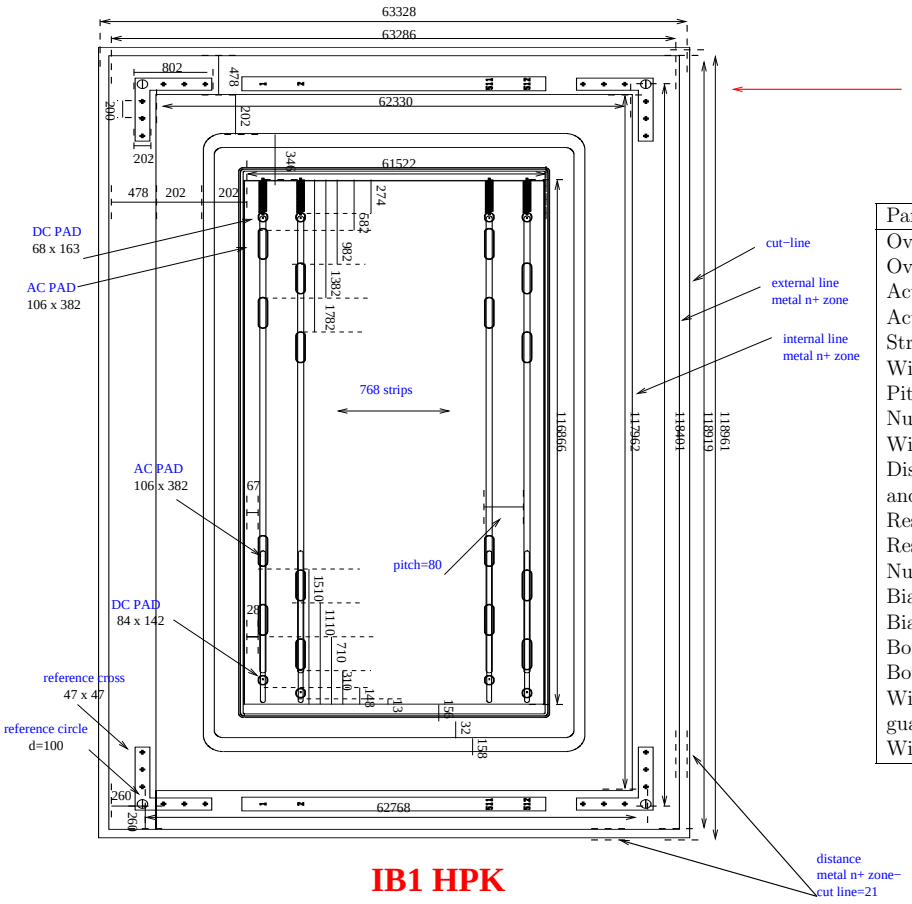

Figure 26: Schematics of the mask design for the IB1 detector

Dimensions on the sketch are
all relative to the metal layer
(except for the external cut−line)

Parameter	Value (μm)
Overall width (after cutting)	63328
Overall lenght (after cutting)	118961
Active area width	61540
Active area lenght	116885
Strip lenght	116825
Width of strip p+ zone	20
Pitch	80
Number of strips	768
Width of metal strip	28
Distance between end of strip's p+ zone and horizontal part of guard ring	30
Resistor height	326
Resistor width	70
Number of squares in a resistor	450
Bias pad height (aperture in passivation)	128
Bias pad width (aperture in passivation)	62
Bonding pad height (aperture in passivation)	364
Bonding pad width (aperture in passivation)	88
Width of the n zone between the edge of first guard ring p+ zone and n+ zone	300
Width of n+ zone	490

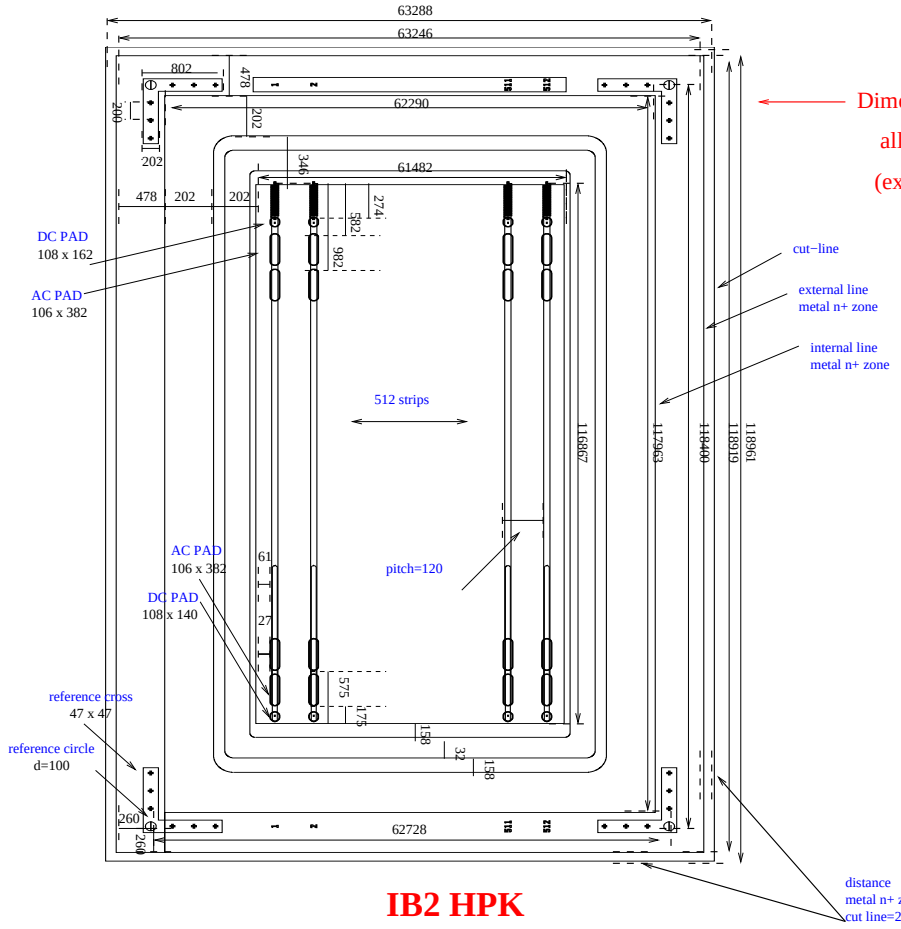

Dimensions on the sketch are all relative to the metal layer (except for the external cut−line)

Parameter	Value (μm)
Overall width (after cutting)	63288
Overall lenght (after cutting)	118961
Active area width	61500
Active area lenght	116885
Strip lenght	116823
Width of strip p+ zone	30
Pitch	120
Number of strips	512
Width of metal strip	40
Distance between end of strip's p+ zone and horizontal part of guard ring	31
Resistor height	326
Resistor width	70
Number of squares in a resistor	450
Bias pad height(*)	128
Bias pad width (*)	88
Bonding pad height (*)	360
Bonding pad width (*)	88
Width of the n zone between the edge of first guard ring p+ zone and n+ zone	250
Width of n+ zone	450

(*) dimension of the aperture in the passivation layer

Figure 27: Schematics of the mask design for the IB2 detector

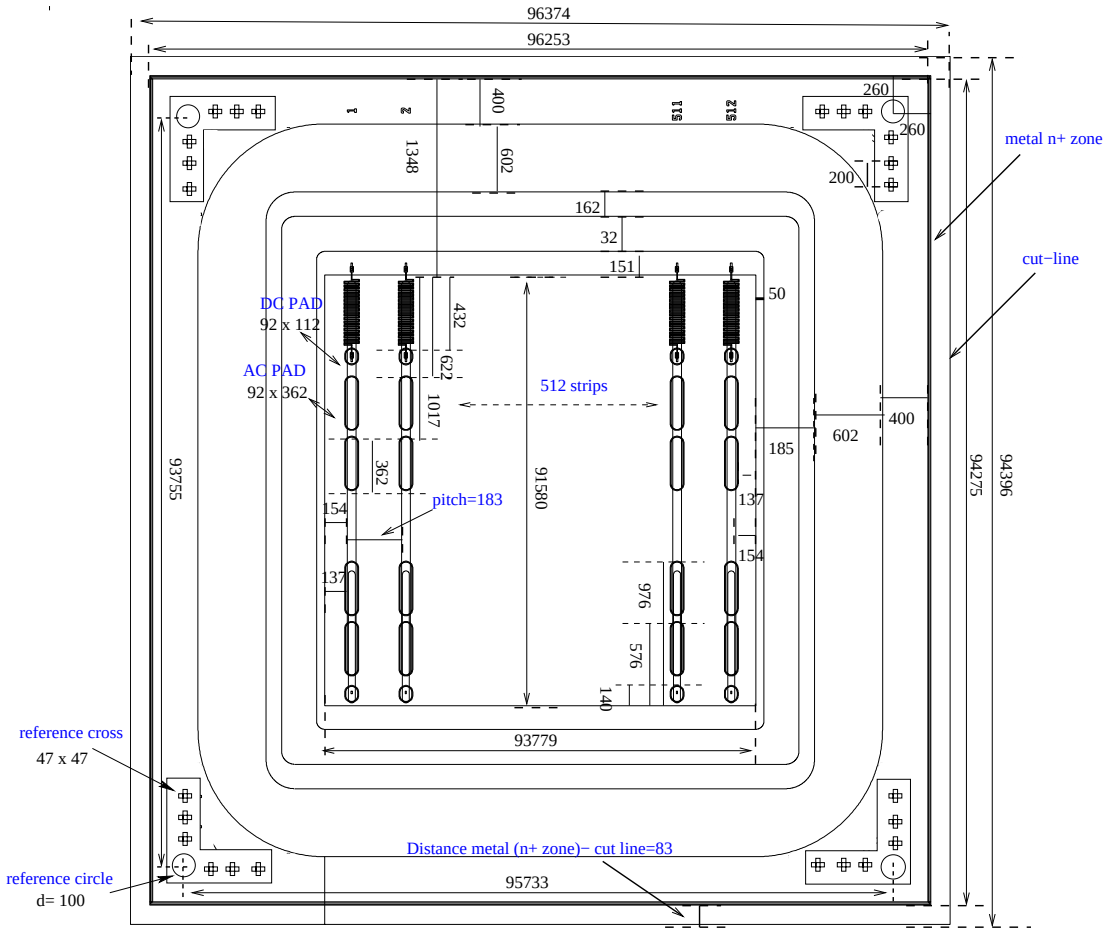

Figure 28: Schematics of the mask design for the OB1 detector

OB1 ST

Dimensions in the sketch are referred to the metal layer (except for the external line)

Parameter	Value (μm)
Overall widht (after cutting)	96374
Overall lenght (after cutting)	94396
Active area width	93869
Active area lenght	91571
Strip lenght	91108
Width of strip p^+ zone	30
Pitch	122
Number of strips	768
Width of metal strip	40
Distance between end of strip p^+ zone and horizontal part of bias ring (lower side)	29
Distance between end of strip p^+ zone and horizontal part of bias ring (upper side)	433
Bias pad height (*)	100
Bias pad width (*)	80
Bonding pad height (*)	350
Bonding pad width (*)	80
Distance between the edge of guard ring p^+ zone and n^+ zone	700
Width of the n^+ zone	410

(*) Dimensions are referred to the opening in the passivation layer

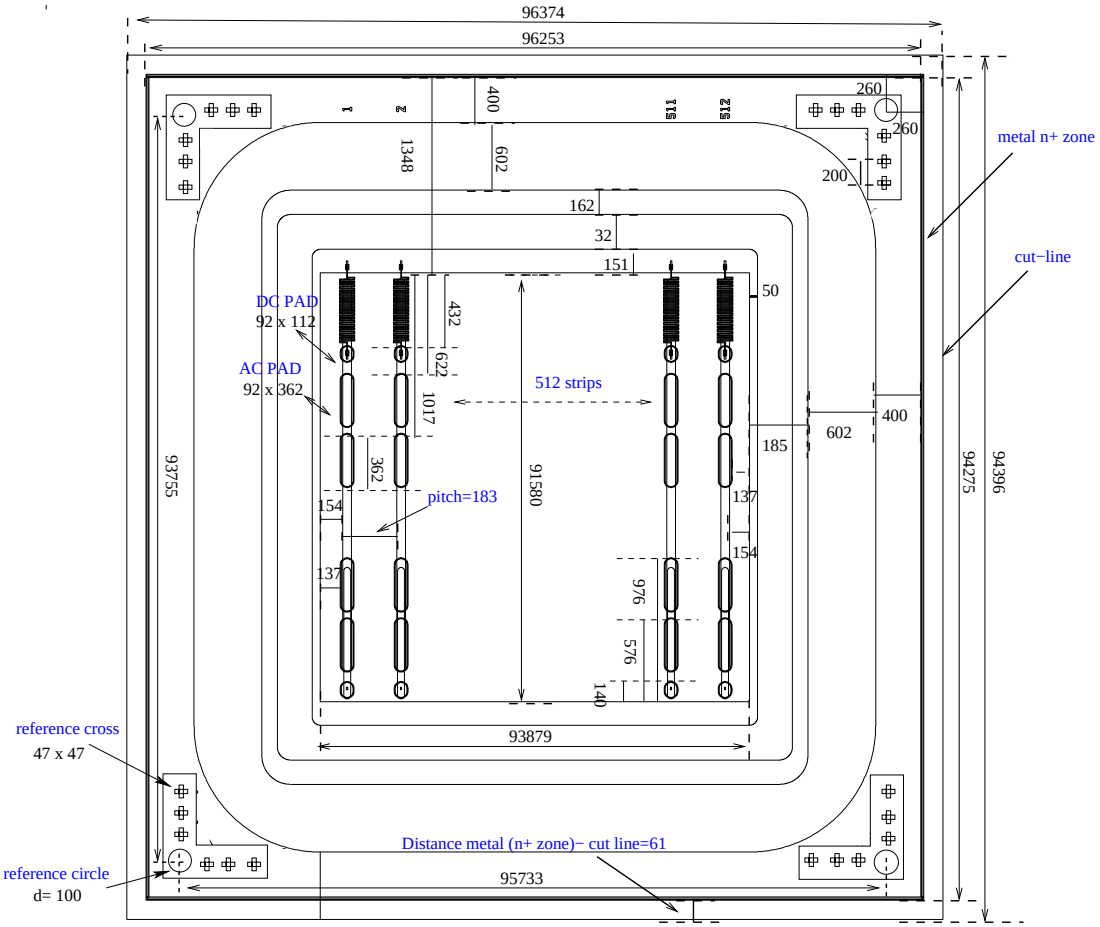

Figure 29: Schematics of the mask design for the OB2 detector

OB2 ST

Dimensions in the sketch are referred to the metal layer (except for the external line)

Parameter	Value (μm)
Overall widht (after cutting)	96374
Overall lenght (after cutting)	94396
Active area width	93869
Active area lenght	91571
Strip lenght	91108
Width of strip p^+ zone	46
Pitch	183
Number of strips	512
Width of metal strip	58
Distance between end of strip p^+ zone and horizontal part of bias ring (lower side)	29
Distance between end of strip p^+ zone and horizontal part of bias ring (upper side)	433
Bias pad height (∗)	102
Bias pad width (∗)	82
Bonding pad height (∗)	352
Bonding pad width (∗)	82
Distance between the edge of guard ring p^+ zone and n^+ zone	700
Width of the n^+ zone	410

(*) Dimensions are referred to the opening in the passivation layer

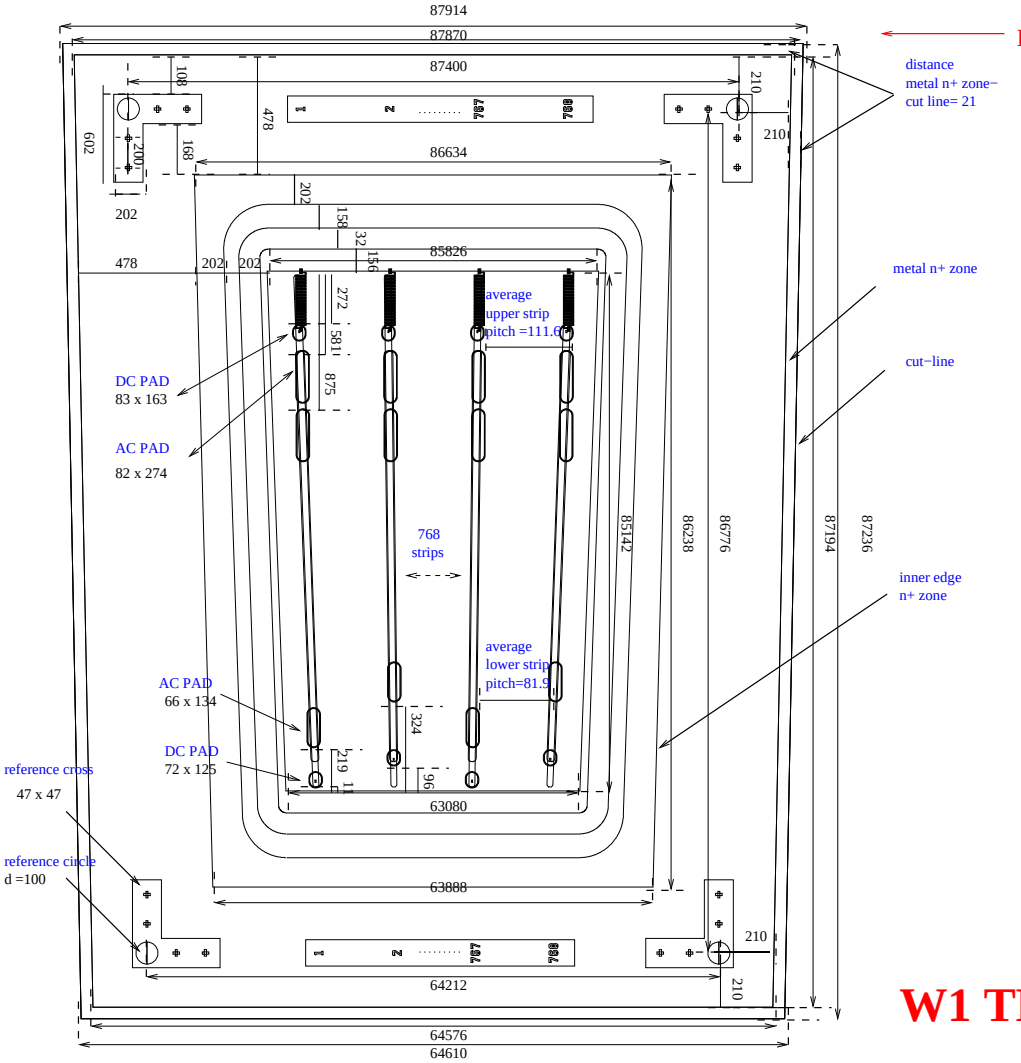

Dimensions on the sketch are all relative to the metal layer (except for the external cut line)

Parameter	Value (μm)
Overall width (after cutting)	64610 −87914
Overall lenght (after cutting)	87236
Active area width	63100 − 85848
Active area lenght	85160
Strip lenght	85100
Width of strip p+ zone	20 −28
Average strip pitch	81.94 − 111.59
Number of strips	768
Width of metal strip	28 − 36
Distance between end of strip's p+ zone and horizontal part of guard ring	30
Resistor height	400
Resistor width	70
Number of squares in a resistor	450
Bias pad height, upper side (*)	128
Bias pad width, upper side (*)	62
Bonding pad height, upper side (*)	258
Bonding pad width, upper side (*)	65
Bias pad height, lower side (*)	90
Bias pad width, lower side (*)	66
Bonding pad height, lower side (*)	118
Bonding pad width, lower side (*)	50
Pitch for upper side bias pads (**)	111.60
Pitch for bonding pads, first upper row (**)	111.60
Pitch for bonding pads, second upper row (**)	111.33
Pitch for bias and bonding pads, lower row (**)	82.07
Width of the n zone between the edge of first guard ring p+ zone and n+ zone	300
Width of n+ zone	450

(*) aperture in the passivation layer
(**) Bias and bond pads have constant pitches but the first one in each group of 16 (8) in the upper (lower) side is adjusted to keep the contact with the corresponding strip.

W1 TEC HPK

Figure 30: Schematics of the mask design for the W1 TEC detector

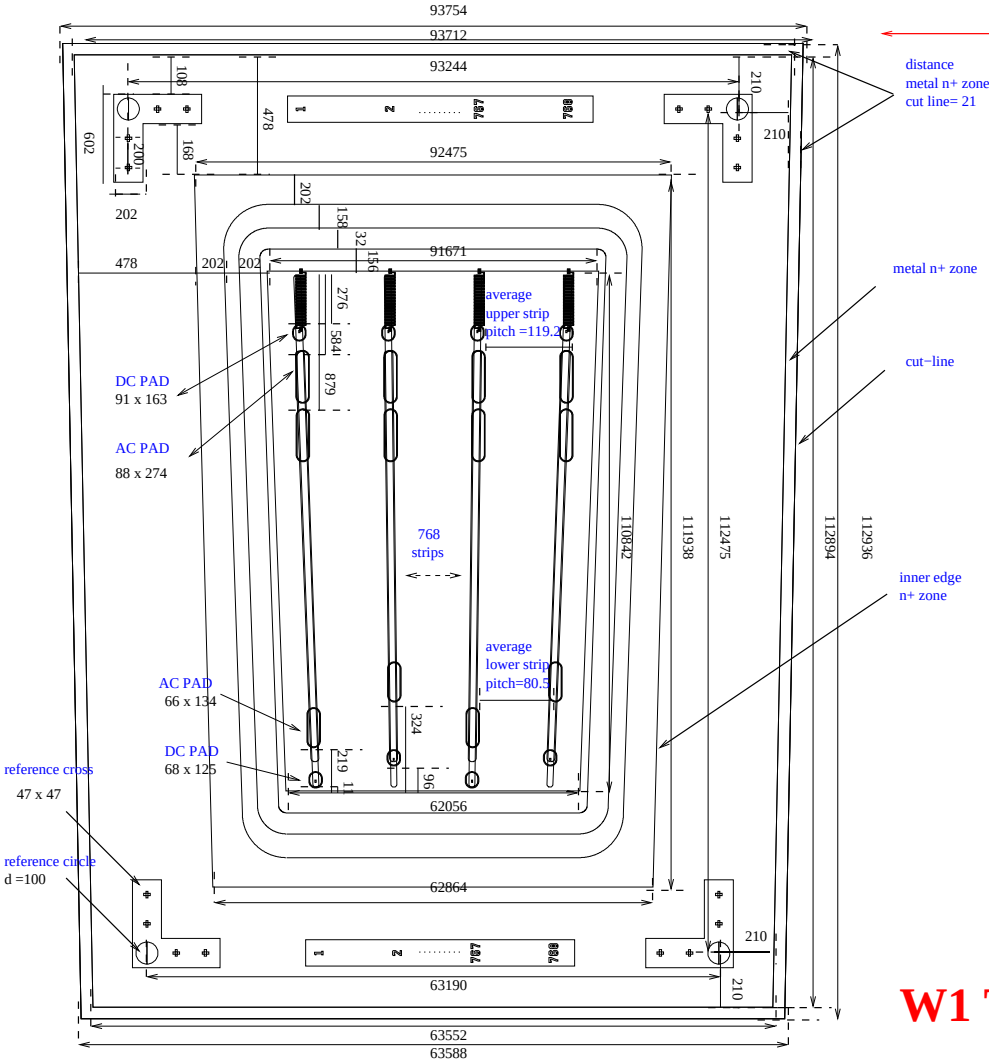

Dimensions on the sketch are all relative to the metal layer (except for the external cut line)

Parameter	Value (μm)
Overall width (after cutting)	63588 −93754
Overall lenght (after cutting)	112936
Active area width	62076 − 91688
Active area lenght	110858
Strip lenght	110800
Width of strip p+ zone	20 −30
Average strip pitch	80.5 − 119.2
Number of strips	768
Width of metal strip	30 − 40
Distance between end of strip's p+ zone and horizontal part of guard ring	30
Resistor height	400
Resistor width	70
Number of squares in a resistor	450
Bias pad height, upper side (*)	128
Bias pad width, upper side (*)	70
Bonding pad height, upper side (*)	258
Bonding pad width, upper side (*)	72
Bias pad height, lower side (*)	90
Bias pad width, lower side (*)	62
Bonding pad height, lower side (*)	118
Bonding pad width, lower side (*)	50
Pitch for upper side bias pads (**)	119.2
Pitch for bonding pads, first upper row (**)	119.2
Pitch for bonding pads, second upper row (**)	118.9
Pitch for bias and bonding pads, lower row (**)	80.71
Width of the n zone between the edge of first guard ring p+ zone and n+ zone	300
Width of n+ zone	450

(*) aperture in the passivation layer
(**) Bias and bond pads have constant pitches but the first one in each group of 16 (8) in the upper (lower) side is adjusted to keep the contact with the corresponding strip.

W1 TID HPK

Figure 31: Schematics of the mask design for the W1 TID detector

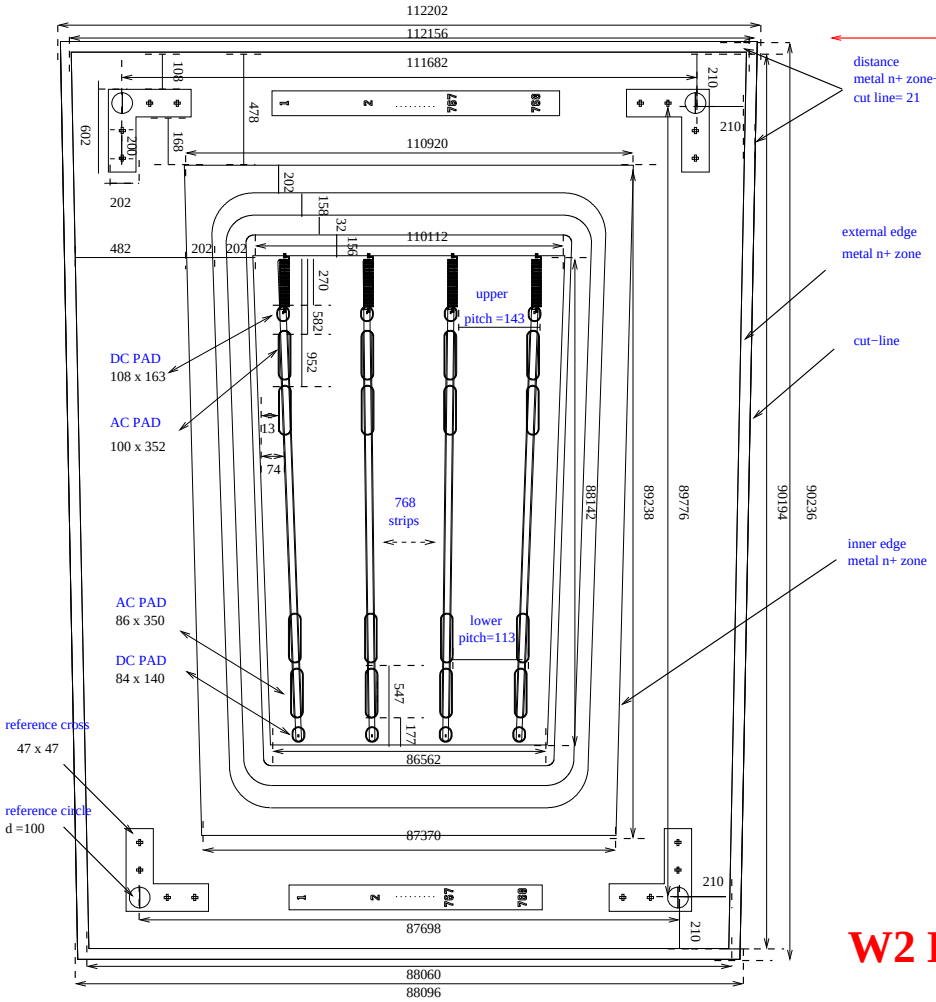

Dimensions on the sketch are all relative to the metal layer (except for the external cut line)

Parameter	Value (μm)
Overall width (after cutting)	88096 −112202
Overall lenght (after cutting)	90236
Active area width	86580 − 110132
Active area lenght	88160
Strip lenght	88100
Width of strip p+ zone	28 − 36
Pitch	113 − 143
Number of strips	768
Width of metal strip	36 − 46
Distance between end of strip's p+ zone and horizontal part of guard ring	30
Resistor height	400
Resistor width	70
Number of squares in a resistor	450
Bias pad height, top (*)	128
Bias pad width, top (*)	88
Bonding pad height, top (*)	334
Bonding pad width, top (*)	82
Bias pad height, bottom (*)	104
Bias pad width, bottom (*)	64
Bonding pad height, bottom (*)	334
Bonding pad width, bottom (*)	70
Pitch for lower side bias pads (**)	112.77
Pitch for bonding pads, first lower row (**)	112.77
Pitch for bonding pads, second lower row (**)	112.77
Pitch for upper side bias pads (**)	142.97
Pitch for bonding pads, first upper row (**)	142.97
Pitch for bonding pads, second upper row (**)	142.90
Width of the n zone between the edge of first guard ring p+ zone and n+ zone	300
Width of n+ zone	450

(*) Aperture in the passivation layer
(**) Bias and bond pads have constant pitches but the first one in each group of 16 is adjusted to keep the contact with the relative strip.

W2 HPK

Figure 32: Schematics of the mask design for the W2 detector

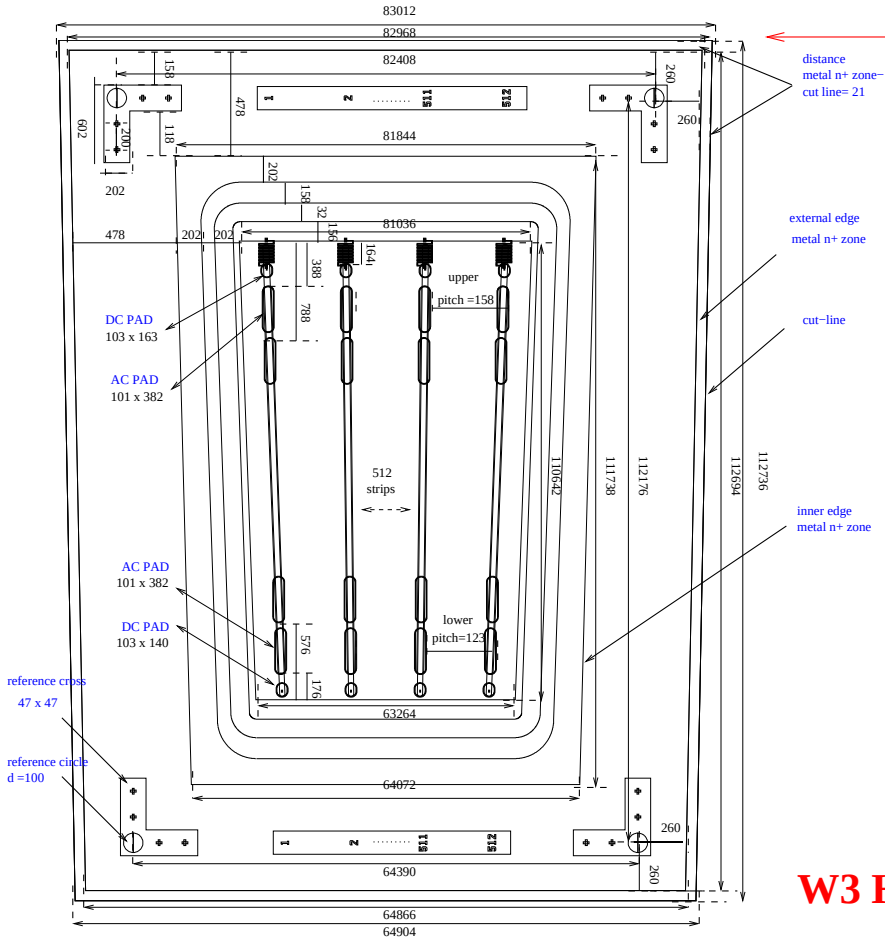

Dimensions on the sketch are all relative to the metal layer (except for the external cut line)

Parameter	Value (μm)
Overall width (after cutting)	64904 — 83012
Overall lenght (after cutting)	112736
Active area width	63282 — 81055
Active area lenght	110660
Strip lenght	110578
Width of strip p+ zone	31 — 39
Pitch	123 — 158
Number of strips	512
Width of metal strip	41 — 51
Distance between end of strip's p+ zone and horizontal part of guard ring	30
Resistor height	200
Resistor width	120
Number of squares in a resistor	450
Bias pad height, top (*)	128
Bias pad width, top (*)	83
Bonding pad height, top (*)	364
Bonding pad width, top (*)	83
Bias pad height, bottom (*)	105
Bias pad width, bottom (*)	83
Bonding pad height, bottom (*)	364
Bonding pad width, bottom (*)	83
Pitch for lower side bias pads	123.33
Pitch for bonding pads, first lower row	123.45
Pitch for bonding pads, second lower row	123.57
Pitch for upper side bias pads	158.06
Pitch for bonding pads, first upper row	158.06
Pitch for bonding pads, second upper row	157.83
Width of the n zone between the edge of first guard ring p+ zone and n+ zone	300
Width of n+ zone	450

(*) aperture in the passivation layer

W3 HPK

Figure 33: Schematics of the mask design for the W3 detector

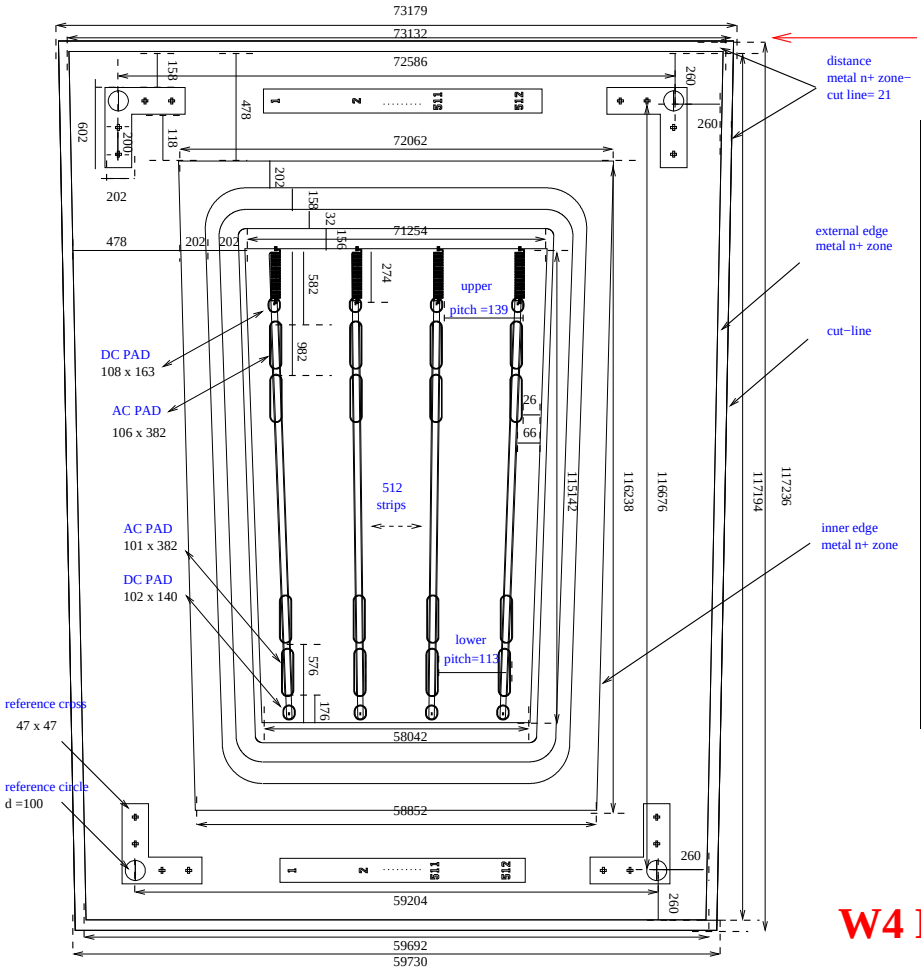

Figure 34: Schematics of the mask design for the W4 detector

Dimensions on the sketch are all relative to the metal layer (except for the external cut line)

Parameter	Value (μm)
Overall width (after cutting)	59730 – 73179
Overall lenght (after cutting)	117236
Active area width	58060 – 71272
Active area lenght	115160
Strip lenght	115100
Width of strip p+ zone	28 – 35
Pitch	113 – 139
Number of strips	512
Width of metal strip	36 – 45
Distance between end of strip's p+ zone and horizontal part of guard ring	30
Resistor height	400
Resistor width	70
Number of squares in a resistor	450
Bias pad height, top (*)	128
Bias pad width, top (*)	88
Bonding pad height, top (*)	364
Bonding pad width, top (*)	88
Bias pad height, bottom (*)	105
Bias pad width, bottom (*)	81
Bonding pad height, bottom (*)	364
Bonding pad width, bottom (*)	83
Pitch for lower side bias pads	113.32
Pitch for bonding pads, first lower row	113.32
Pitch for bonding pads, second lower row	113.41
Pitch for upper side bias pads	138.92
Pitch for bonding pads, first upper row	138.92
Pitch for bonding pads, second upper row	138.83
Width of the n zone between the edge of first guard ring p+ zone and n+ zone	300
Width of n+ zone	450

(*) aperture in the passivation layer

W4 HPK

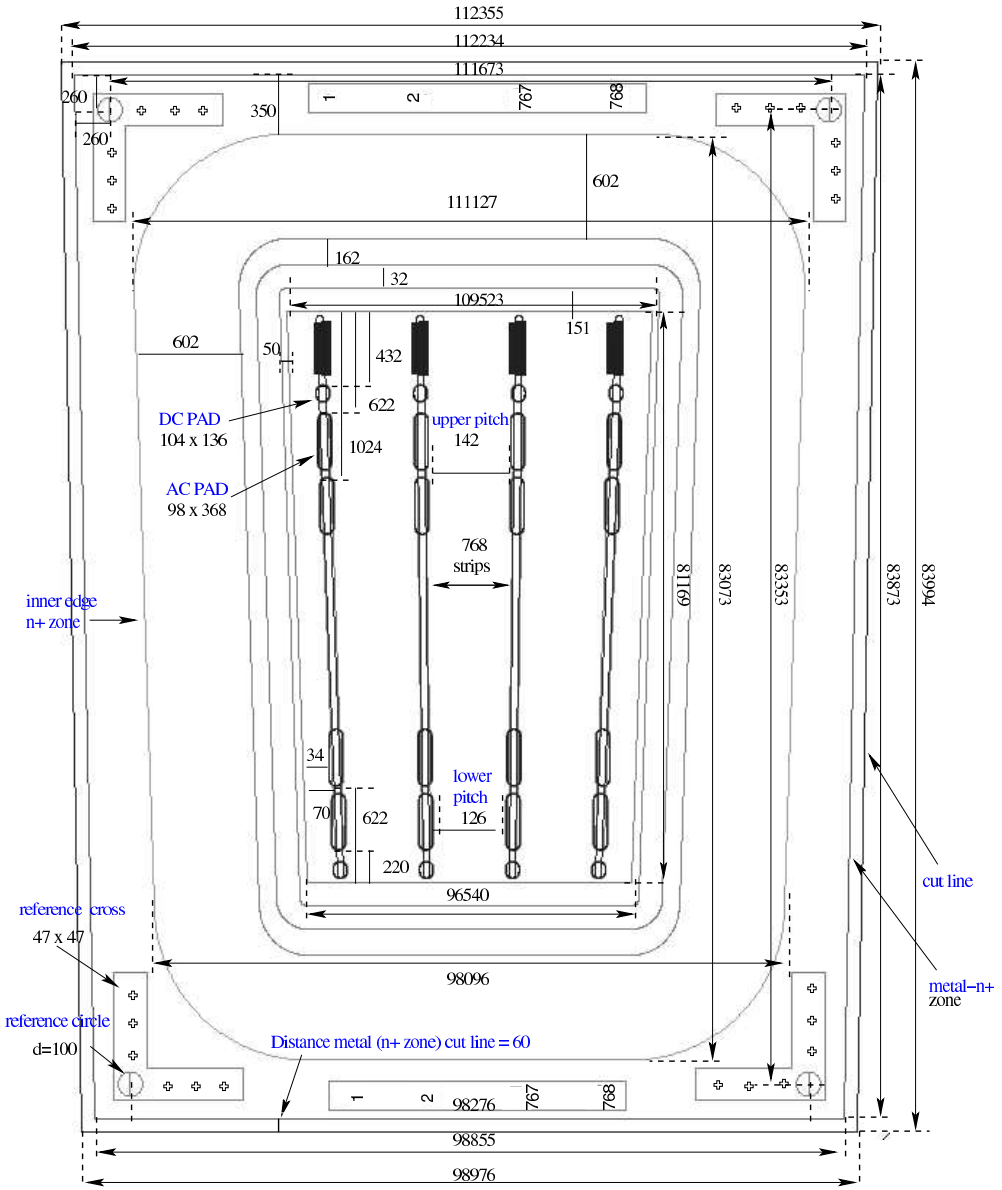

Figure 35: Schematics of the mask design for the W5A detector

W5A ST

Dimensions on the sketch are referred to the metal layer (except for the external cut line).

Parameter	Value (μm)
Overall width (after cutting)	98976-112355
Overall lenght (after cutting)	83994
Active area width	96540-109523
Active area lenght	81169
Strip lenght	80606
Width of strip p^+ zone	31-36
Pitch	126-142
Number of strips	768
Width of metal strip	41-46
Distance between end of strip p^+ zone and horizontal part of bias ring (lower side)	29
Distance between end of strip p^+ zone and horizontal part of bias ring (upper side)	433
Bias pad height (*)	102
Bias pad width (*)	94
Bonding pad height (*)	358
Bonding pad width (*)	88
Pitch for bias pads (lower side)	125.63
Pitch for bonding pads, first lower row	125.66
Pitch for bonding pads, second lower row	125.75
Pitch for bias pads (upper side)	142.35
Pitch for bonding pads, first upper row	142.35
Pitch for bonding pads, second upper row	142.25
Distance between the edge of guard ring p^+ zone and n^+ zone	700
Width of the n^+ zone	410

(*) Dimensions are referred to the opening in the passivation layer

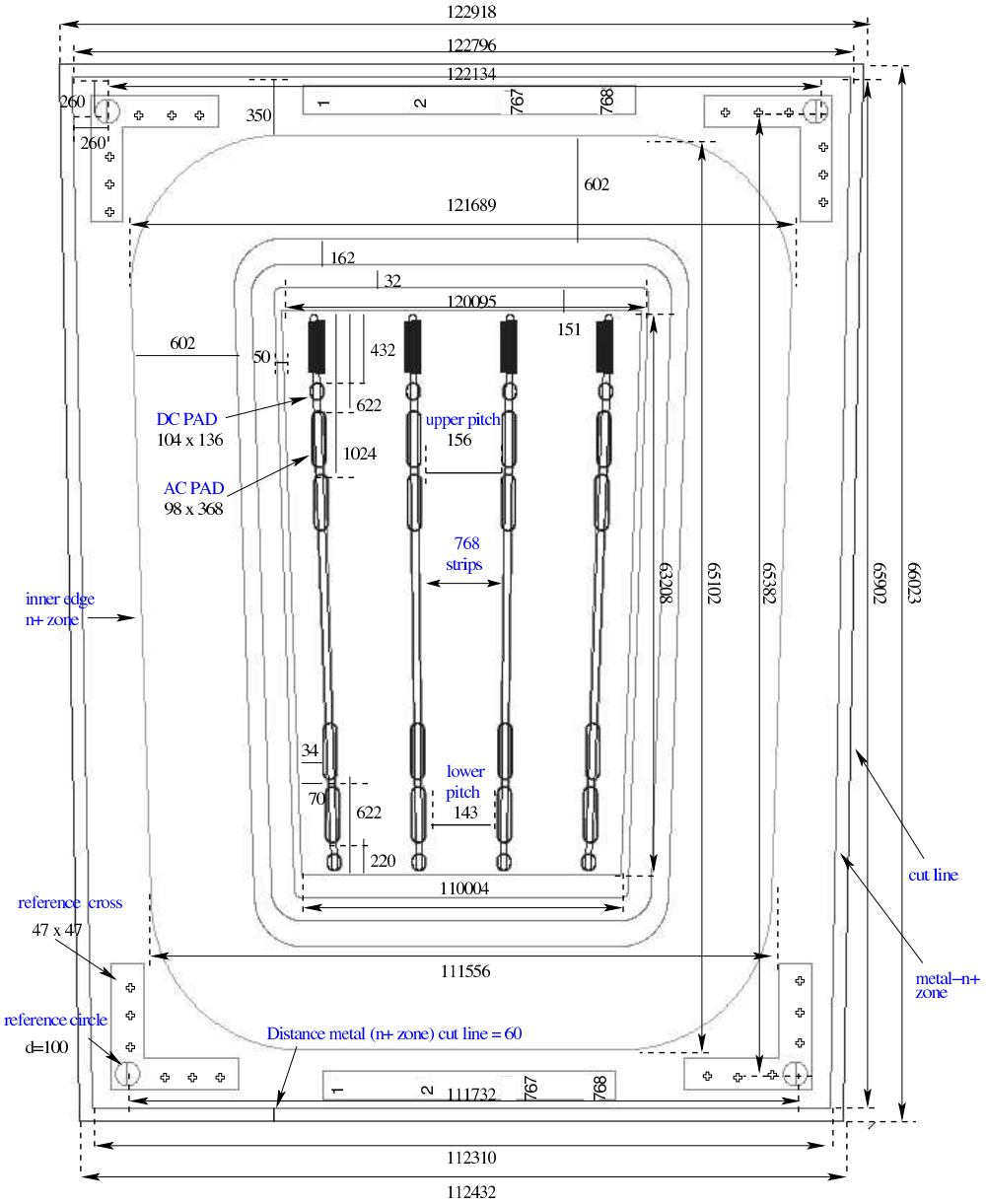

Figure 36: Schematics of the mask design for the W5B detector

W5B ST

Dimensions on the sketch are referred to the metal layer (except for the external cut line).

Parameter	Value (μm)
Overall width (after cutting)	112432-122918
Overall lenght (after cutting)	66023
Active area width	109994-120085
Active area lenght	63198
Strip lenght	62736
Width of strip p^+ zone	36-39
Pitch	143-156
Number of strips	768
Width of metal strip	46-51
Distance between end of strip p^+ zone and horizontal part of bias ring (lower side)	29
Distance between end of strip p^+ zone and horizontal part of bias ring (upper side)	433
Bias pad height (*)	102
Bias pad width (*)	94
Bonding pad height (*)	358
Bonding pad width (*)	88
Pitch for bias pads (lower side)	143.1
Pitch for bonding pads, first lower row	143.15
Pitch for bonding pads, second lower row	143.3
Pitch for bias pads (upper side)	156.13
Pitch for bonding pads, first upper row	156.13
Pitch for bonding pads, second upper row	156.1
Distance between the edge of guard ring p^+ zone and n^+ zone	700
Width of the n^+ zone	410

(*) Dimensions are referred to the opening in the passivation layer

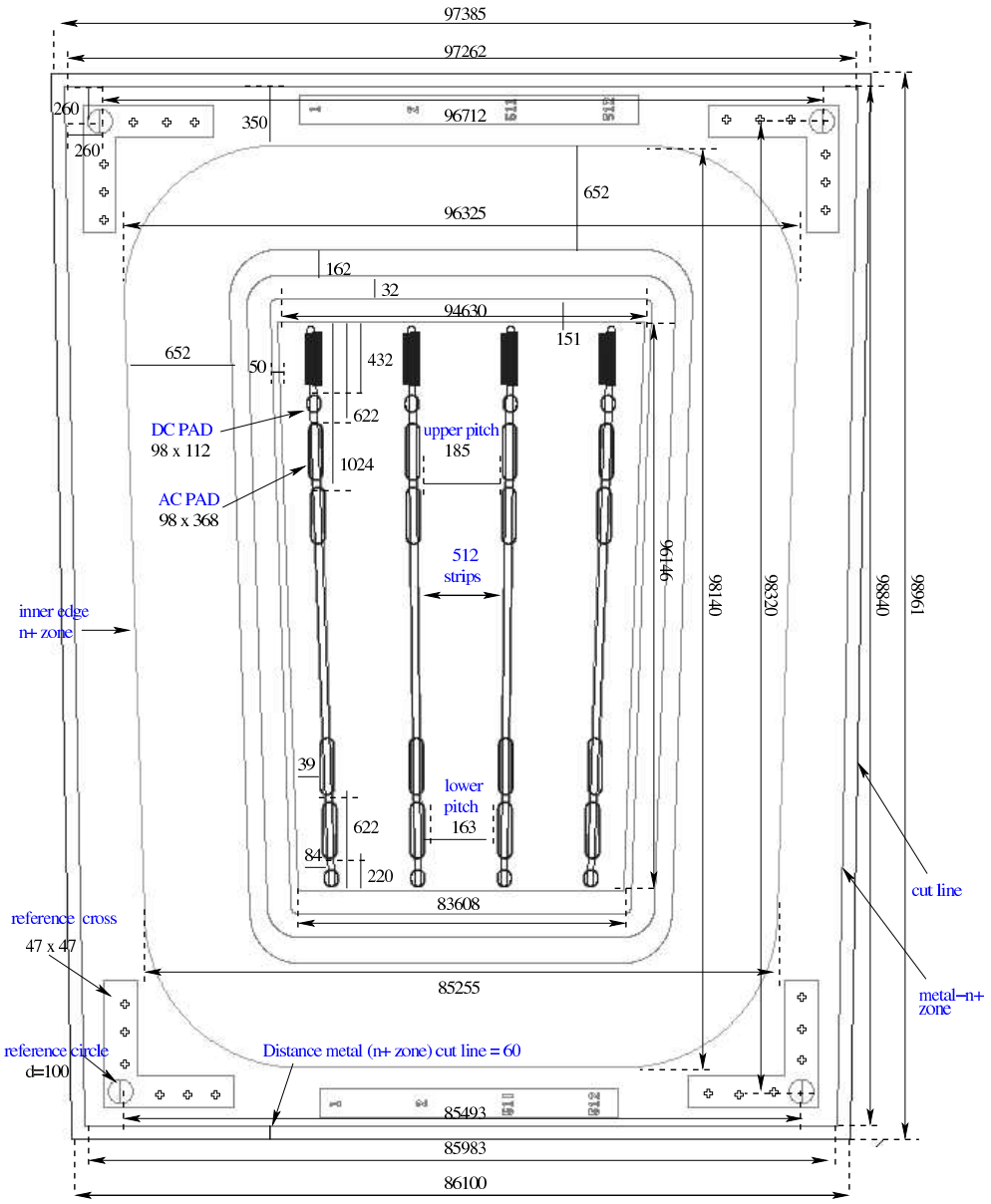

Figure 37: Schematics of the mask design for the W6A detector

W6A ST

Dimensions on the sketch are referred to the metal layer (except for the external cut line).

Parameter	Value (μm)
Overall width (after cutting)	86100-97385
Overall lenght (after cutting)	98961
Active area width	83600-94620
Active area lenght	96136
Strip lenght	95573
Width of strip p^+ zone	41-46
Pitch	163-185
Number of strips	512
Width of metal strip	53-60
Distance between end of strip p^+ zone and horizontal part of bias ring (lower side)	29
Distance between end of strip p^+ zone and horizontal part of bias ring (upper side)	433
Bias pad height (*)	102
Bias pad width (*)	88
Bonding pad height (*)	358
Bonding pad width (*)	88
Pitch for bias pads (lower side)	163.2
Pitch for bonding pads, first lower row	163.2
Pitch for bonding pads, second lower row	163.4
Pitch for bias pads (upper side)	184.6
Pitch for bonding pads, first upper row	184.6
Pitch for bonding pads, second upper row	184.5
Distance between the edge of guard ring p^+ zone and n^+ zone	700
Width of the n^+ zone	410

(*) Dimensions are referred to the opening in the passivation layer

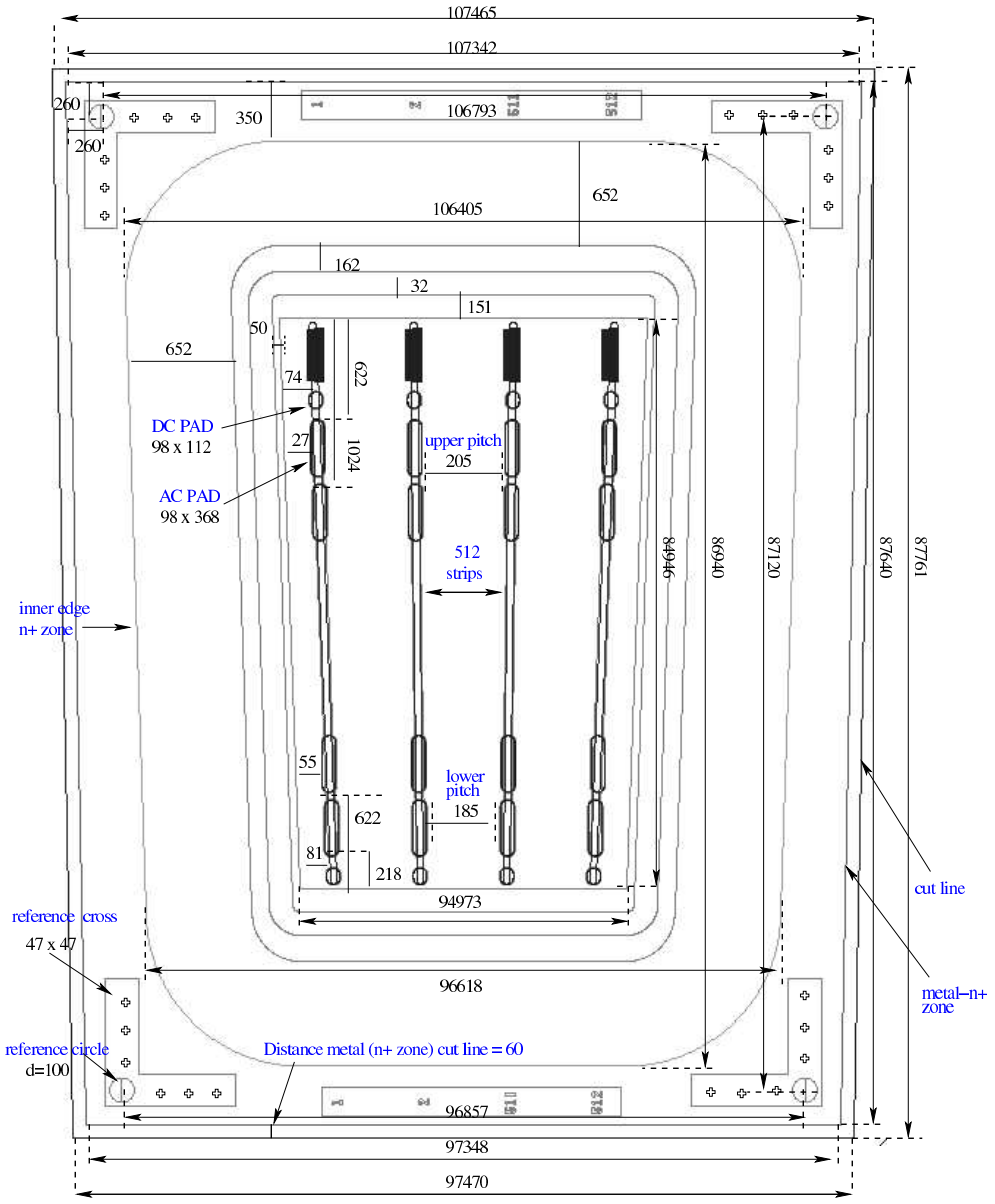

Figure 38: Schematics of the mask design for the W6B detector

W6B ST

Dimensions on the sketch are referred to the metal layer (except for the external cut line).

Parameter	Value (μm)
Overall widht	97470-107465
Overall lenght	87761
Active area width	94963-104701
Active area lenght	84936
Strip lenght	84475
Width of strip p^+ zone	46-51
Pitch	185-205
Number of strips	512
Width of metal strip	60-67
Distance between end of strip p^+ zone and horizontal part of bias ring (lower side)	29
Distance between end of strip p^+ zone and horizontal part of bias ring (upper side)	433
Bias pad height (*)	102
Bias pad width (*)	88
Bonding pad height (*)	358
Bonding pad width (*)	88
Pitch for bias pads (lower side)	185.5
Pitch for bonding pads, first lower row	185.5
Pitch for bonding pads, second lower row	185.6
Pitch for bias pads (upper side)	204.4
Pitch for bonding pads, first upper row	204.4
Pitch for bonding pads, second upper row	204.2
Distance between the edge of guard ring p^+ zone and n^+ zone	700
Width of the n^+ zone	410

(*) Dimensions are referred to the opening in the passivation layer

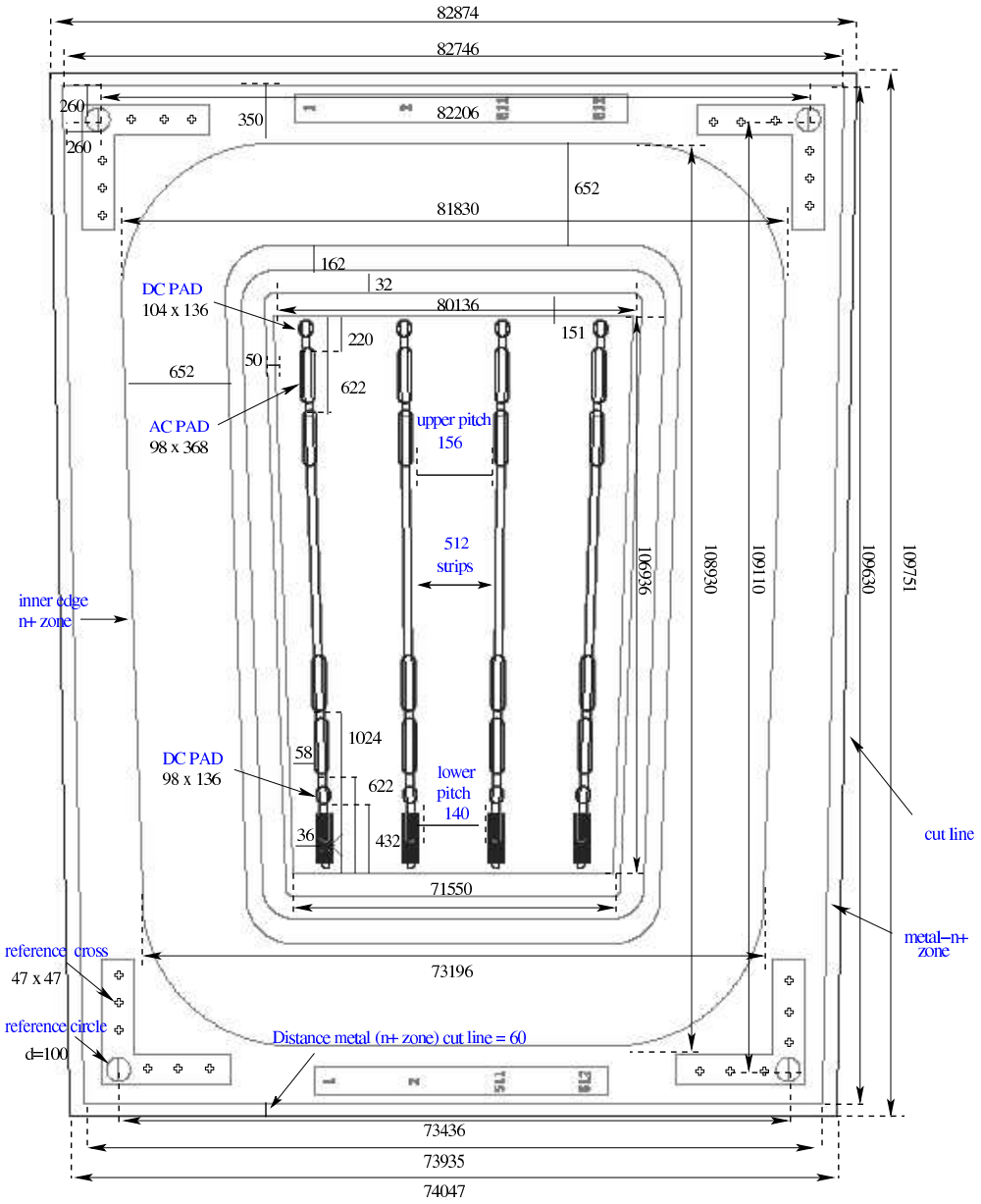

Figure 39: Schematics of the mask design for the W7A detector

W7A ST

Dimensions on the sketch are referred to the metal layer (except for the external cut line).

Parameter	Value (μm)
Overall width (after cutting)	74047-82874
Overall lenght (after cutting)	109751
Active area width	71540-80126
Active area lenght	106926
Strip lenght	106464
Width of strip p^+ zone	35-39
Pitch	140-156
Number of strips	512
Width of metal strip	45-51
Distance between end of strip p^+ zone and horizontal part of bias ring (upper side)	29
Distance between end of strip p^+ zone and horizontal part of bias ring (lower side)	433
Bias pad height (*)	102
Bias pad width (*)	94
Bonding pad height (*)	358
Bonding pad width (*)	88
Pitch for bias pads (lower side)	139.67
Pitch for bonding pads, first lower row	139.67
Pitch for bonding pads, second lower row	139.7
Pitch for bias pads (upper side)	156.35
Pitch for bonding pads, first upper row	156.35
Pitch for bonding pads, second upper row	156.34
Distance between the edge of guard ring p^+ zone and n^+ zone	700
Width of the n^+ zone	410

(*) Dimensions are referred to the opening in the passivation layer

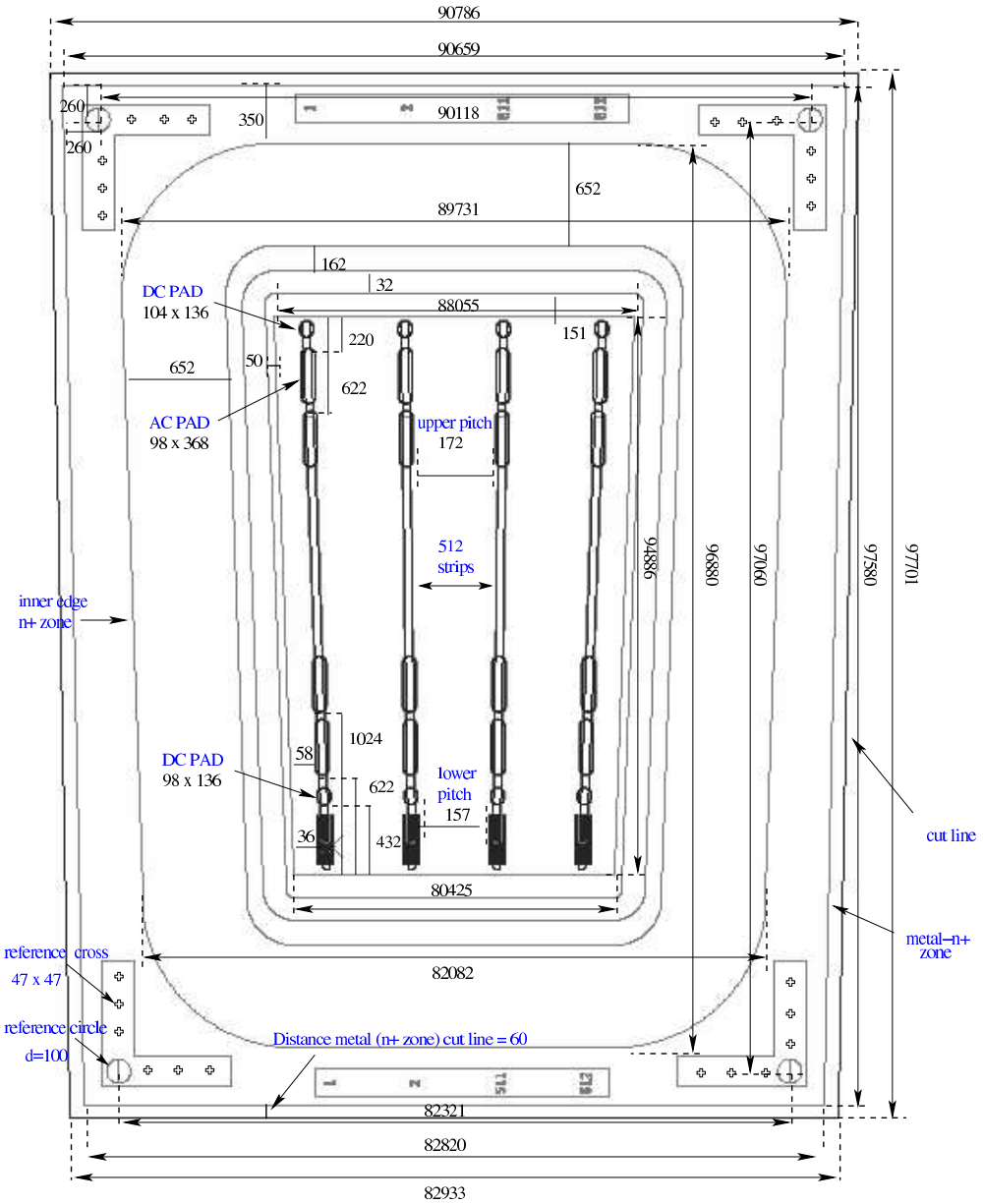

Figure 40: Schematics of the mask design for the W7B detector

W7B ST

Dimensions on the sketch are referred to the metal layer (except for the external cut line).

Parameter	Value (μm)
Overall width (after cutting)	82923-90786
Overall lenght (after cutting)	97701
Active area width	80415-88045
Active area lenght	94876
Strip lenght	94414
Width of strip p^+ zone	39-43
Pitch	156-172
Number of strips	512
Width of metal strip	51-55
Distance between end of strip p^+ zone and horizontal part of bias ring (upper side)	29
Distance between end of strip p^+ zone and horizontal part of bias ring (lower side)	433
Bias pad height (*)	102
Bias pad width (*)	88
Bonding pad height (*)	358
Bonding pad width (*)	88
Pitch for bias pads (lower side)	157
Pitch for bonding pads, first lower row	157
Pitch for bonding pads, second lower row	157.01
Pitch for bias pads (upper side)	171.76
Pitch for bonding pads, first upper row	171.76
Pitch for bonding pads, second upper row	171.74
Distance between the edge of guard ring p^+ zone and n^+ zone	700
Width of the n^+ zone	410

(*) Dimensions are referred to the opening in the passivation layer